Ministry of Higher Education and Scientific Research

National Higher School of Statistics and Applied Economics

(E.N.S.S.E.A)

Dissertation Submitted in Partial Fulfillment of the Requirements for the Degree of Master in Statistics and Applied Economics

Major: Statistics and Data Science

Theme

Wildfire Risk Assessment Using Long Short-Term Memory (LSTM) and Explainable Artificial Intelligence (XAI) Case Study: Mediterranean Basin (2006–2022)

Presented by:

Yacine KIBBOUA

Supervised by:

Dr Ayoub ASRI

2024/2025

Ministry of Higher Education and Scientific Research

National Higher School of Statistics and Applied Economics

(E.N.S.S.E.A)

Dissertation Submitted in Partial Fulfillment of the Requirements for the Degree of Master in Statistics and Applied Economics

Major: Statistics and Data Science

Theme

Wildfire Risk Assessment Using Long Short-Term Memory (LSTM) and Explainable Artificial Intelligence (XAI) Case Study: Mediterranean Basin (2006–2022)

Presented by:

Yacine KIBBOUA

Supervised by:

Dr Ayoub ASRI

2024/2025

Dedication

To you :

My Parents,

My Sister and Brother,

My Family,

My Dear Friends,

My Teachers,

and **to anyone reading**,

May your path be filled with purpose, growth, and fulfillment.

Acknowledgements

In the name of Allah, the Most Gracious, the Most Merciful.

All praise is due to Allah, whose mercy, guidance, and countless blessings have sustained me throughout this journey. Without Allah, none of this would have been possible.

I am especially grateful to Dr. Ayoub Asri for his guidance, encouragement, and thoughtful feedback, which have been invaluable throughout this work. Thank you for your time, your patience, your trust in my ideas, and for all you have taught me over these past three years.
I would also like to extend my sincere thanks to the jury members for their time and consideration in evaluating this thesis.

To my teachers, past and present, and to my school and its entire community, I express my deepest appreciation.
Finally, to my friends, and to everyone who has offered a kind word, a helping hand, or a moment of encouragement along the way: thank you.

Abstract

Wildfires in the Mediterranean Basin are intensifying due to the combined impacts of climate change and human activity, creating an urgent need for accurate and interpretable risk assessment tools. This study proposes a novel framework that integrates Long Short-Term Memory (LSTM) networks with Explainable Artificial Intelligence (XAI) methods to predict wildfire ignitions while maintaining model transparency. Leveraging the Mesogeos dataset (2006–2022), which includes meteorological, environmental, and anthropogenic variables, the LSTM model demonstrates strong predictive performance (AUPRC = 89%; Recall = 87.5%), effectively capturing temporal dependencies in fire drivers. Interpretability analyses using Integrated Gradients and Permutation Feature Importance reveal that meteorological factors, particularly those linked to temperature and moisture dynamics, are the dominant predictors, aligning with established fire ecology. The integration of deep learning and interpretability yields a valuable decision-support tool for wildfire management, bridging the gap between computational precision and operational applicability in fire-prone landscapes.

Keywords: Wildfire risk, Explainable AI, Deep learning, Temporal modeling, Mediterranean ecosystems, Predictive analytics

Résumé

Les feux de végétation dans le bassin méditerranéen s'intensifient sous l'effet combiné du changement climatique et des activités humaines, ce qui crée un besoin urgent d'outils d'évaluation des risques à la fois précis et interprétables. Cette étude propose un cadre méthodologique innovant combinant des réseaux de neurones Long Short-Term Memory (LSTM) avec des techniques d'Intelligence Artificielle Explicable (XAI) pour prédire les départs de feu tout en assurant la transparence du modèle. En exploitant le jeu de données Mesogeos (2006–2022), qui intègre des variables météorologiques, environnementales et anthropiques, le modèle LSTM présente de solides performances prédictives (AUPRC = 89% ; rappel = 87,5 %), en capturant efficacement les dépendances temporelles des facteurs de risque. Les analyses d'interprétabilité, fondées sur les méthodes Integrated Gradients et Permutation Feature Importance, révèlent que les facteurs météorologiques, en particulier ceux liés à la température et à l'humidité, sont les principaux prédicteurs, en cohérence avec les connaissances écologiques établies sur les régimes de feu. L'intégration de l'apprentissage profond et de l'interprétabilité fournit un outil d'aide à la décision précieux pour la gestion des incendies, comblant le fossé entre la précision computationnelle et l'applicabilité opérationnelle dans les paysages à risque.

Mots-clés : Risque de feu de végétation, Intelligence Artificielle Explicable, Apprentissage profond, Modélisation temporelle, Écosystèmes méditerranéens, Analyse prédictive

Summary

List of Figures

List of Tables

List of Abbreviations

AI: Artificial Intelligence

AUC: Area Under the Curve (Receiver Operating Characteristic)

AUPRC: Area Under the Precision-Recall Curve

BPTT: Backpropagation Through Time

CO: Carbon Monoxide

CO_2: Carbon Dioxide

DFMC: Dead Fuel Moisture Content

DL: Deep Learning

DNN: Deep Neural Network

EDA: Exploratory Data Analysis

EFFIS: European Forest Fire Information System

FCCS: Fuel Characteristic Classification System

FMC: Fuel Moisture Content

FPR: False Positive Rate

GD: Gradient Descent

GHG: Greenhouse Gas

GIS: Geographic Information System

ICS: Incident Command System

IG: Integrated Gradients

LAI: Leaf Area Index

LFMC: Live Fuel Moisture Content

LOCF: Last Observation Carried Forward

LSTM: Long Short-Term Memory

MSE: Mean Squared Error

NDVI: Normalized Difference Vegetation Index

NOCB: Next Observation Carried Backward

NO_x: Nitrogen Oxides

PCA: Principal Component Analysis

PFI: Permutation Feature Importance

$PM_{2.5}$: Fine Particulate Matter

ReLU: Rectified Linear Unit

RH: Relative Humidity

RMSE: Root Mean Squared Error

RNN: Recurrent Neural Network

SGD: Stochastic Gradient Descent

SMI: Soil Moisture Index

SSRD: Surface Solar Radiation Downwards

t-SNE: t-Distributed Stochastic Neighbor Embedding

TPR: True Positive Rate

UMAP: Uniform Manifold Approximation and Projection

VOCs: Volatile Organic Compounds

VPD: Vapor Pressure Deficit

WUI: Wildland-Urban Interface

XAI: Explainable Artificial Intelligence

General Introduction

Wildfires represent one of the most destructive natural hazards worldwide, with far-reaching ecological, economic, and societal consequences. In fire-prone regions, such as the Mediterranean Basin, wildfires have long been a natural component of ecosystem dynamics. However, in recent decades, their behavior has changed dramatically. A combination of anthropogenic climate change, land use shifts, vegetation transitions, and increasing human expansion into wildland areas has intensified the frequency, scale, and severity of wildfires. These changes have led to unprecedented impacts: ecosystems are being pushed beyond their resilience thresholds, communities are suffering more frequent evacuations and property loss, and emergency services are increasingly overwhelmed during fire seasons.

The Mediterranean Basin is particularly vulnerable due to its hot, dry summers, flammable vegetation, and densely populated landscapes. According to recent studies, the region has experienced a marked rise in the number of large fires and the total area burned, trends that are projected to worsen under future climate scenarios. As a result, improving wildfire prediction capabilities has become a high priority for both researchers and practitioners. Effective early warning systems are essential not only for triggering timely evacuations and resource mobilization but also for designing proactive land and vegetation management strategies aimed at mitigating fire risk.

Yet, despite considerable progress in fire science and modeling, wildfire prediction remains a major challenge. The main difficulty lies in the complexity of fire dynamics, which emerge from the interplay of meteorological variables, fuel conditions, topography, and human influences. Traditional models, including statistical and rule-based systems, often struggle to capture these high-dimensional and dynamic relationships. Moreover, many existing operational tools rely on static fire danger indices, such as the Fire Weather Index (FWI), which, although useful, are often derived from simplified assumptions and do not fully leverage the spatio-temporal structure of available data.

Machine learning (ML) has emerged as a promising alternative by enabling data-driven risk assessments that learn complex input-output relationships from historical fire records. Algorithms such as random forests and gradient-boosted trees have demonstrated strong predictive performance in many settings. However, a common limitation of these models is that they frequently treat inputs as static snapshots, ignoring temporal dependencies that are critical for understanding ignition risk, especially in dynamic weather regimes. In response, deep learning models, particularly Recurrent Neural Networks (RNNs) and their variants such as Long Short-Term Memory (LSTM) networks, have shown great potential in modeling sequential dependencies and evolving fire conditions over time.

Nevertheless, the adoption of deep learning in operational wildfire management is still limited by one key issue: *interpretability*. LSTM models, like many deep neural networks, are considered "black boxes" due to their complex internal structure. This opacity undermines trust and limits their utility for practitioners who need clear explanations to justify decisions in high-stakes environments. Therefore, the current state of wildfire prediction is caught between two competing imperatives: maximizing

predictive accuracy through advanced models while ensuring transparency and interpretability for actionable risk communication.

Against this backdrop, the central research problem emerges: **How can we develop a wildfire risk assessment framework that simultaneously achieves high predictive performance, accounts for temporal dynamics, and provides interpretable insights to domain experts?** This question captures the fundamental trade-off at the heart of modern AI-driven disaster forecasting and motivates the need for novel solutions that bridge the gap between complex model architectures and operational usability.

This dissertation explores the integration of **Explainable Artificial Intelligence (XAI)** techniques with **Long Short-Term Memory (LSTM)** networks to address this challenge. Specifically, we focus on the Mediterranean Basin from 2006 to 2022, a region where seasonal fire risk is both high and increasingly variable. We apply two complementary XAI methods, Integrated Gradients (IG) and Permutation Feature Importance (PFI), to gain insight into model behavior and to identify which factors drive ignition predictions. The study is guided by two core hypotheses:

1. **Hypothesis 1**: An LSTM-based model will outperform non-sequential models due to its ability to learn and exploit temporal dependencies in the data.
2. **Hypothesis 2**: Interpretability techniques will reveal that short-term weather features are the dominant predictors, aligning with known fire ecology.

This research contributes a novel, transparent, and time-aware modeling framework for wildfire risk assessment. The ultimate goal is to empower decision-makers, such as emergency responders, forest managers, and policymakers, with accurate predictions and also clear, evidence-based explanations that support targeted intervention and resource allocation.

The dissertation is organized as follows: **Chapter 1** provides the foundational context on wildfires, detailing ignition mechanisms, ecological consequences, human drivers, and evolving trends. This chapter also highlights key challenges in modeling wildfire occurrence and behavior. **Chapter 2** introduces core concepts in artificial intelligence, with a particular focus on machine learning and deep learning. Special attention is given to the structure and functionality of LSTM networks, as well as the theoretical underpinnings of explainable AI. **Chapter 3** presents the empirical study, including data preprocessing, feature engineering, model training, and evaluation. It also contains a detailed interpretation of the results using both IG and PFI, offering a nuanced understanding of the drivers of fire risk as learned by the model. The dissertation concludes with a synthesis of findings, a discussion of their implications for real-world wildfire management, and suggestions for future work aimed at improving both prediction and interpretability in environmental AI applications.

CHAPTER 1:

Fundamentals Of Wildfires

Chapter 1

Fundamentals Of Wildfires

Introduction

Wildfires are complex natural threats that profoundly impact ecosystems, human societies, and global systems. Their behavior results from the intricate interplay of chemical, meteorological, ecological, and land management factors, requiring a multidisciplinary understanding. This chapter provides a foundational overview of wildfires, starting with definitions and classifications, and exploring the core principles of ignition, spread, and progression. Key concepts such as the Fire Triangle, Fire Behavior Triangle, and heat transfer mechanisms are discussed in detail. The chapter also examines the effects of wildfires on ecosystems, human health, the environment, and economies, emphasizing their destructive potential. Finally, it highlights the latest trends in wildfire occurrences and their increasing significance due to climate change. It also outlines contemporary strategies for wildfire prevention, mitigation, and management, establishing the knowledge base for future discussions on wildfire risk prediction.

1 Overview of Wildfires

1.1 Wildfires Definition

Wildfires arise from the dynamic interactions between environmental factors, such as climate, vegetation, and topography, and human activity, including land use, policies, and socioeconomic conditions. Their occurrence, patterns, and impact vary depending on these interacting forces, making them a complex phenomenon. As formally defined by the Food and Agriculture Organization (FAO), *"A wildfire is any unplanned and uncontrolled vegetation fire that, regardless of ignition source, may negatively affect social, economic, or environmental values, and require suppression response or other action according to agency policy"* (Food & Organization, 2024).

The terminology used to describe wildfires differs among experts and researchers based on disciplinary perspectives, sector-specific concerns, and individual interpretations. Common descriptions include Disturbance, Natural Hazard, Climate-Sensitive Hazard, and Socio-Ecological Hazard. The latter is particularly fitting, as it accounts for both the environmental and human factors influencing wildfires, as well as their broad effects. While wildfires play a key role in maintaining certain ecological processes, they often pose significant threats, leading to environmental degradation and risks to human

communities (Tedim & Leone, 2020).

1.2 Wildfires Classification

Wildfires can be classified based on the context in which they occur. Examples include terms such as rural fire, wildland-urban interface fire, farming fire, and even seasonally influenced terms like summer fire. Another classification method distinguishes wildfires based on their fire behavior, with three main types: ground fire, surface fire, and crown fire (Huidobro, Giessen, & Burns, 2024).

- **Ground fires:** Burning beneath the surface, ground or smoldering fires typically occur during periods of prolonged drought. They smolder for extended periods, spread slowly, and can be challenging to detect and extinguish due to their deep-seated nature (Gupta, Agrawal, & Chauhan, 2022).
- **Surface fires:** Also known as crawling fires, these fires burn along the floor, consuming grass, shrubs, fallen leaves, and other surface vegetation. They typically spread at moderate speeds and produce lower-intensity flames compared to crown fires (Gupta et al., 2022).
- **Crown fires:** Typically ignited by surface fires, crown fires spread through the canopy, consuming vegetation above the surface. They can be classified into two types:
  - **Passive crown fires:** where individual trees or small groups of trees burn (a process called torching), but fire does not spread continuously through the canopy.
  - **Active crown fires:** which create a solid wall of flame extending from the surface through the upper canopy. These fires rapidly spread from one tree crown to another, often resulting in intense, uncontrollable wildfire behavior (Gupta et al., 2022).

2 Wildfire Dynamics and Progression:

2.1 Basic Fire chemistry:

Fire is the visible effect of a chemical reaction known as combustion, in which a fuel,a substance capable of burning, reacts rapidly with oxygen, releasing heat and light and often producing a glowing, gaseous flame at the ignition point.

Combustion is the reverse of photosynthesis. Photosynthesis allows plants to absorb carbon dioxide and water, converting them into glucose and oxygen using sunlight. This process stores energy within the chemical bonds of glucose, facilitating plant growth and releasing oxygen into the atmosphere. Conversely, combustion involves burning plant matter in the presence of oxygen, releasing the stored energy as heat, and emitting carbon dioxide back into the atmosphere (Leavell, Berger, Fitzgerald, & Parker, 2017).

2.2 Fire Triangle

At the heart of wildfire formation lies the fire triangle or combustion triangle, a concept highlighting the three essential components needed for a fire to start and sustain itself: heat, fuel, and oxygen (Figure 1.1). The absence of any of these components will prevent a fire from igniting or cause it to extinguish (Madrzykowski, 2012).

Figure 1.1: The Fire Triangle.

Source: NatureBridge Retrieved March 5

2.2.1 Heat: The Ignition Source

In the context of wildfires, heat refers to the energy necessary to raise the fuel temperature to its ignition point. This energy can come from various sources, broadly categorized as either natural or human-caused. While natural causes have historically played a role in shaping ecosystems, human-induced fires have become increasingly prevalent, often resulting in more severe wildfire events.

a) Natural Ignitions Sources

Several natural processes can ignite wildfires, especially under favorable environmental conditions:

- **Lightning Strikes:** Lightning strikes are a major natural cause of wildfire ignition, often sparking fires in dry vegetation and contributing to large-scale fire spread (Song, Xu, Li, & Oppong, 2024).
- **Volcanic Activity:** Volcanic activity can trigger wildfires by igniting surrounding vegetation through lava flows and ejecting hot debris (Rahman, White, & Ma, 2024).
- **Spontaneous Combustion:** Although rare, spontaneous combustion can ignite wildfires under specific conditions. This occurs when organic material, such as accumulated dead leaves and decaying vegetation, undergoes microbial decomposition, generating heat. If sufficient fuel and oxygen are present, the material can reach its ignition point, starting a fire without an external source (Prestemon et al., 2013).

b) Human Caused Ignition Sources

A significant portion of wildfires are caused by human activities, either intentionally or accidentally, making them a major contributor to wildfire occurrences worldwide (Farid et al., 2024). Some of the most common triggers include:

- **Arson:** The deliberate act of intentionally setting fire to land or property, often with malicious intent, is a major criminal cause of wildfires (Prestemon et al., 2013).

- **Campfires and Outdoor Burning:** Unattended campfires and poorly managed outdoor burning of debris or waste can quickly spread beyond control, igniting nearby vegetation (Prestemon et al., 2013).
- **Discarded Smoking Materials:** Carelessly discarded cigarettes, matches, or other smoking materials can easily ignite dry vegetation, particularly in drought-prone areas (Prestemon et al., 2013).
- **Fireworks:** Fireworks can accidentally ignite vegetation or other flammable materials, especially in hot and windy conditions (Vachula, Nelson, & Hall, 2023).
- **Power Line Failures:** Power lines, especially in strong winds, can spark wildfires by breaking and coming into contact with dry vegetation. Regular maintenance, tree trimming around them, and prompt repairs are crucial for reducing this risk (Jahn, Urban, & Rein, 2022).

2.2.2 Fuel: The Material That Burns

Fuels encompass all combustible materials capable of sustaining a fire. From an ecological perspective, these materials consist of both living and dead organic matter, collectively referred to as biomass. Biomass includes vegetation such as trees, shrubs, leaves, and plant debris that accumulate in ecosystems over time (Keane, 2015).

Building upon the definition of fuels, it is essential to consider the concept of *fuelbed*. The fuelbed represents the broadest level of fuel classification. It encompasses all forms of biomass within a given area, along with their spatial distribution (Keane, 2015).

The fuelbed is generally divided into three vertical fuel layers: ground, surface, and canopy fuels.

a) Ground Fuels

Ground fuels consist of all organic material found below the ground line, which is typically located just beneath the litter. The most prevalent type of ground fuel is duff, a compact layer formed through the progressive decomposition of surface fuels. As this process occurs along a gradient, duff is often divided into two layers: the upper duff (fermentation layer or F layer), where some fuel particles remain identifiable, and the lower duff (humus layer or H layer), where decomposition is more advanced, making particles unrecognizable (Keane, 2015).

Due to its dense structure, duff retains moisture more effectively, making it slower to dry and more resistant to ignition. Its high mineral content further reduces fire spread, as minerals do not burn and instead absorb heat, limiting the proportion of combustible material. As a result, duff primarily burns through smoldering rather than flaming combustion. However, when the upper duff dries sufficiently, it can contribute to surface fire spread in combination with litter fuels (Keane, 2015).

While duff is a key component of ground fuels, plant roots also play a role, though they are often overlooked. Roots are generally not considered significant in fire intensity due to their uneven spatial distribution and underground position. However, burning roots can pose challenges in fire suppression, as they can remain active for extended periods, often going undetected and later reigniting surface fires under favorable environmental conditions. Additionally, the loss of root systems due to combustion can destabilize soil and contribute to tree mortality, further altering fire-affected landscapes.(Keane, 2015).

Figure 1.2: The elements of a typical fuelbed.

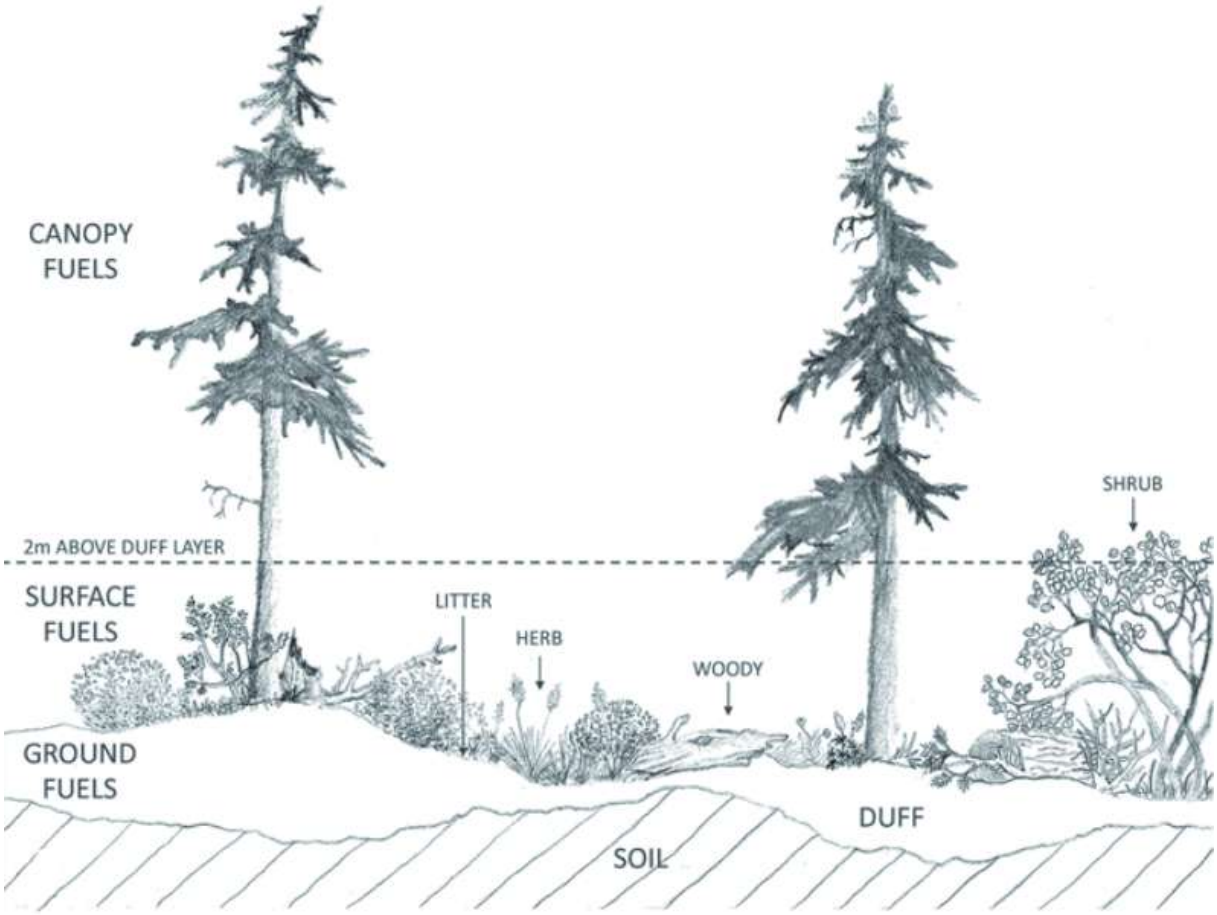

Source: (Keane, 2015), p.4

b) Surface Fuels

Surface fuels consist of all combustible material resting on or near the ground, typically within 2 meters of the surface. These fuels are the primary carriers of fire in many ecosystems, influencing fire spread, intensity, and duration (Lutes, Keane, & Caratti, 2009). Surface fuels include litter, which consists of dead plant material such as fallen leaves, needles, and small twigs that dry quickly and ignite easily. Herbaceous plants, such as grasses and forbs, are also highly flammable, especially when dry, allowing fire to spread rapidly across open landscapes. Shrubs, if tall enough, can act as *ladder fuels*, carrying fire from the surface into the canopy (Figure 1.2). Finally, downed woody debris, including branches, logs, and stumps, takes longer to ignite due to higher moisture content but can burn for extended periods, contributing significantly to fire intensity.

These classifications align with the fuel strata described by Keane (2015) and are essential for accurate fire behavior prediction.

c) Canopy Fuels

Canopy fuels are the biomass above the surface fuel layer, typically at heights exceeding 2 meters. These fuels include both live and dead combustible vegetation found in tree crowns, such as leaves, needles, branches, and suspended dead material (Keane, 2013).

Canopy fuels are often described using quantitative measures (Keane, 2013). One key factor influencing canopy fire behavior is canopy base height, which refers to the lowest point where flammable foliage is present. A lower canopy base height allows surface fires to ignite canopy fuels more easily, increasing the likelihood of tree torching. Canopy fuel load, the total amount of combustible material in the canopy, determines the potential energy release. A higher fuel load provides more burning material, leading to greater heat production and longer fire duration (Keane, 2015).

Another critical characteristic is canopy bulk density, which describes how tightly packed the combustible material is within a given volume of canopy space. A higher bulk density allows flames to spread more easily between tree crowns, sustaining active crown fires. The interplay between these structural properties ultimately determines whether a fire remains at the surface or transitions into a sustained crown fire (Keane, 2015).

Canopy fuels play a key role in wildfire behavior. Their characteristics determine how fires interact with the upper levels of vegetation, influencing fire intensity and spread.

2.2.3 Oxygen: Supporting Combustion

Oxygen is a crucial component of the fire triangle, as it supports the chemical reactions necessary for combustion. Ambient air is composed of approximately 21 percent oxygen, while most fires require at least 16 percent to sustain combustion (Leavell et al., 2017). A fire ignited in an area with little oxygen will support only a small flame, while higher oxygen concentrations result in more vigorous burning. Since atmospheric oxygen is generally abundant, it is rarely the limiting factor in wildfires. Instead, fire behavior is primarily influenced by fuel availability and heat.

2.3 Fire Spread: Heat Transfer Mechanisms

Wildfire spread is governed by four primary mechanisms: conduction, convection, radiation, and solid fuel transport (spotting). Each of these mechanisms plays a distinct role in transferring heat from burning vegetation to adjacent fuel, enabling the fire to sustain and propagate (Sullivan, 2017).

2.3.1 Conduction

Conduction is the process by which heat is transferred through direct contact between materials. Conduction is generally considered a minor mechanism of fire spread in wildfires due to the non-contiguous nature of most vegetative fuels. However, it becomes essential in dense fuels such as logs, tree trunks, and compacted vegetation where heat moves slowly through the material. This internal heat transfer can cause smoldering combustion, allowing fires to persist longer and potentially reignite under the right conditions (Sullivan, 2017).

2.3.2 Convection

Convection refers to the transfer of heat through the movement of gases, primarily air. In wildfires, hot gases produced by combustion rise due to buoyancy[1], forming a convective column. As these gases ascend, they mix with the cooler surrounding air, creating unstable air currents that redistribute heat in multiple directions. This turbulent mixing extends the reach of convective heating, particularly in windy conditions, where hot air is advected forward over unburned fuels, drying and preheating them. These combined effects contribute to erratic fire behavior and accelerate fire spread (Sullivan, 2017).

2.3.3 Radiation

Radiation is the transfer of heat in the form of electromagnetic waves, primarily in the infrared spectrum[2]. Unlike conduction and convection, which require a medium to transfer heat, radiation doesn't need one and can travel through empty space. In wildfires, flames and burning fuels emit radiant energy, which moves in all directions and is absorbed by nearby fuels, preheating and drying them. The efficiency of radiative heat transfer depends on flame temperature, fuel moisture, and the distance between the heat source and the target fuel. Under calm conditions, radiation is often the dominant mechanism of fire spread, particularly in fine fuels, such as grasses and shrubs, which absorb heat quickly and ignite more easily once preheated. However, radiation alone is often insufficient to sustain fire spread in the absence of additional convective or conductive heat transfer (Sullivan, 2017).

2.3.4 Solid Fuel Transport (Spotting)

Spotting is the process by which burning embers, or firebrands, are transported by wind or convection currents to ignite new fires beyond the main fire perimeter. This mechanism significantly enhances fire spread and can occur in two ways: firebrands can be lofted into the atmosphere by a strong convective column and carried downwind, or they can be blown directly from the flame front over short distances. The distance a firebrand travels depends on its size, shape, mass, wind speed, and atmospheric stability (Sullivan, 2017).

Ignited spot fires can outpace the main fire, complicating suppression efforts and increasing the unpredictability of fire behavior. In extreme wildfire events, long-range spotting can transport embers several kilometers ahead of the main fire, allowing flames to cross firebreaks, rivers, and roads, further escalating fire spread (Benson, Roads, & Weise, 2008).

These four mechanisms interact dynamically, influencing the overall behavior of a wildfire. Their relative importance varies based on environmental conditions such as fuel type, wind speed, humidity, and topography.

2.4 Fire Behavior Triangle

The Fire Behavior Triangle expands upon the traditional Fire Triangle by incorporating three key environmental factors that influence how wildfires spread and behave (Figure 1.3). Unlike the Fire Triangle, which explains the basic requirements for combustion, the Fire Behavior Triangle provides insight into the conditions that control fire intensity, direction, and duration.

[1] **Buoyancy** is the upward force that causes heated air to rise because it is less dense than the cooler air around it.
[2] **The infrared spectrum** consists of electromagnetic waves that are invisible to the human eye but can be felt as heat when they reach a surface.

Figure 1.3: The Fire Behavior Triangle

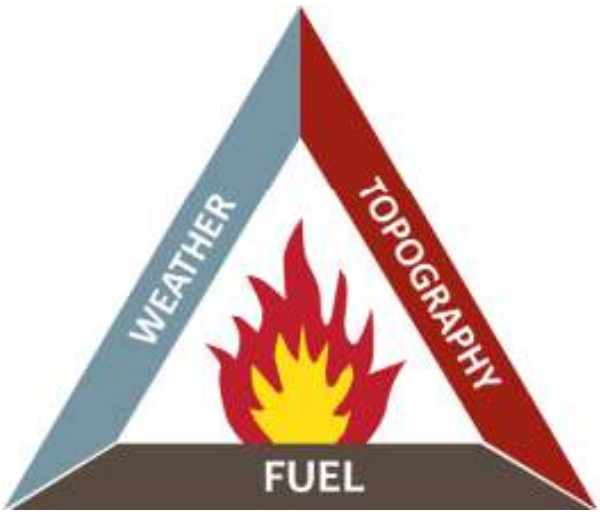

Source: NatureBridge Retrieved March 13

2.4.1 Fuel

Fuels are the only common component between the two fire triangles, underscoring their fundamental role in both ignition and fire spread. Various fuel characteristics influence how a fire develops, including:

a) Fuel Moisture Content

Fuel moisture content (FMC) is a critical factor in wildfire behavior, influencing ignition likelihood, fire spread, and overall intensity. It represents the ratio of water weight to dry weight in a given fuel sample, typically expressed as a percentage. FMC is categorized into live fuel moisture content (LFMC) and dead fuel moisture content (DFMC), each responding differently to environmental conditions. LFMC is regulated by plant physiology, varying with seasonal growth cycles, soil moisture availability, and atmospheric humidity. In contrast, DFMC is influenced by external factors such as temperature, relative humidity, and precipitation, as dead fuels no longer retain the ability to manage their moisture levels actively. Dry fuels ignite more readily, while higher moisture content increases the energy required for combustion, slowing fire spread and reducing fire intensity(Z. Xu et al., 2024).

b) Fuel Load

Fuel load refers to the total amount of combustible material present in an area, typically measured in tons per hectare. It determines the energy available for combustion, directly influencing fire intensity[3] and duration. Higher fuel loads contribute to more extreme fire behavior by providing greater amounts of flammable biomass. Fuel load is generally classified into fine fuels, such as grasses and leaves, which ignite quickly and promote rapid fire spread, and coarse fuels, including logs and large branches, which burn more slowly but sustain long-duration smoldering fires. Fuel load assessments are essential for predicting fire severity[4] (Z. Xu et al., 2024).

[3]Fire **intensity** is a measure of the heat energy released during flaming combustion.
[4]Fire **severity** is a measure of a fire's impact on the site, in other words, fire effects.

c) Fuel Type

Fuel type classification is crucial for predicting wildfire behavior, as different vegetation types exhibit distinct combustion properties. Fuels are broadly categorized into grasslands, shrublands, and forests, with further subdivisions based on characteristics such as fuel size, composition, and flammability. Standardized classification systems, including the Fuel Characteristic Classification System (FCCS) and the Canadian Fire Behavior Prediction (FBP) system, systematically assess fuel properties, aiding in fire modeling and risk assessment (Z. Xu et al., 2024).

d) Fuel Continuity

Fuel continuity refers to the spatial distribution of fuels across a landscape, influencing fire spread. It is classified into horizontal continuity, which describes the density and arrangement of fuels on the ground, and vertical continuity, which represents the connection between surface and canopy fuels. High horizontal continuity, such as dense grasslands, enables fire to propagate rapidly, while vertical continuity, often facilitated by ladder fuels like shrubs, allows surface fires to transition into crown fires, increasing fire intensity and complicating suppression efforts (Z. Xu et al., 2024).

2.4.2 Weather

Weather conditions play a pivotal role in wildfire dynamics, with factors such as wind, temperature, humidity, and precipitation significantly influencing fire ignition, spread, and intensity.

a) Wind

Wind plays a crucial role in wildfire behavior by influencing flame shape, heat transfer, and fire spread rate. Strong winds supply oxygen to the combustion zone, intensify flames, and push heat ahead of the fire front, promoting rapid fire growth. Wind-driven fires can spread unpredictably, as gusts create erratic flame movements and loft firebrands over long distances, igniting new spot fires. However, in certain conditions, strong winds can also hinder fire ignition through convective cooling, where air movement disperses heat away from adjacent fuels, preventing them from reaching ignition temperatures. The overall impact of wind depends on its speed, direction, and interaction with terrain and atmospheric stability (Sullivan, 2017).

b) Temperature

High temperatures accelerate fuel drying, reducing moisture content and making vegetation more flammable. Increased evaporation further depletes fuel moisture, enhancing ignition potential and sustaining combustion. Prolonged heat waves amplify these effects, extending dry conditions and lengthening the fire season. As a result, persistent high temperatures create an environment where wildfires ignite more easily and spread rapidly (Benson et al., 2008).

c) Humidity

Humidity influences wildfire behavior by controlling fuel moisture content, which directly affects ignition potential. Under low humidity, vegetation rapidly loses moisture, becoming more flammable and prone to ignition. In contrast, high humidity slows the drying process, making fuels less receptive to burning and reducing fire intensity (Benson et al., 2008).

d) Precipitation

Precipitation influences wildfire behavior by altering fuel moisture content. Adequate rainfall increases fuel moisture, thereby reducing the immediate risk of ignition and fire spread. However, extended periods without precipitation can lead to drought conditions, resulting in drier fuels that are more prone to ignition and can sustain more intense fires. Seasonal variations in precipitation can also impact wildfire dynamics; for instance, a wet season followed by a dry one can lead to an abundance of vegetation growth that, once dried, serves as additional fuel for wildfires (Benson et al., 2008).

e) Fire-Induced Weather

Under extreme conditions, wildfires can generate their own localized weather systems. These phenomena occur when the intense heat from combustion causes rapid upward air convection, forming *pyrocumulus* and, in more severe cases, *pyrocumulonimbus* clouds. These fire-induced cloud systems can trigger erratic winds, dry lightning, and sudden changes in fire direction (figure 1.4). Pyrocumulonim-

Figure 1.4: Pyrocumulonimbus Clouds

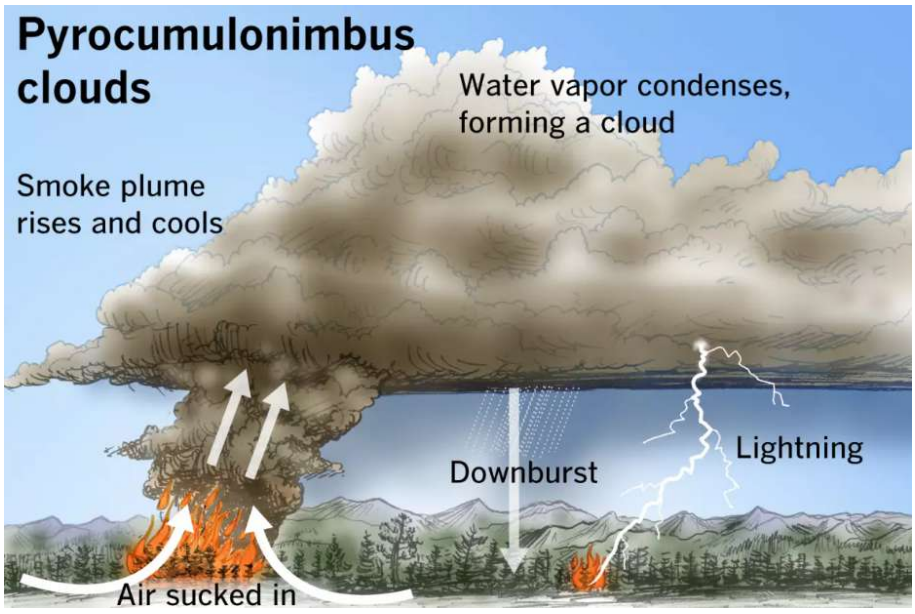

Source: Bureau of Meteorology Retrieved March 16

bus storms produce downdrafts and gust fronts that dramatically increase fire spread and intensity. This interaction between fire and atmosphere establishes a dynamic feedback loop, where the fire modifies local weather conditions, which in turn influence its behavior. These self-reinforcing dynamics make fire progression more unpredictable and hazardous (Fromm et al., 2010).

2.4.3 Topography

Topography refers to the shape and configuration of the landscape, influencing wildfire behavior through three key elements: slope, aspect, and terrain features. Slope steepness is particularly significant as fires tend to move more rapidly uphill due to the preheating of fuels above the fire front through radiation and convection. Steeper slopes increase the rate of spread, while downward slopes can slow fire progression. Operational rules of thumb suggest that for every ten degrees (10°) of slope, the rate of fire spread can increase from a few percent to nearly double (Sullivan, 2017). Aspect, or the direction a slope faces, also affects fire behavior by determining sun exposure and fuel drying rates. South-facing slopes in the Northern Hemisphere[5] typically experience higher temperatures and lower humidity, making them more prone to ignition. Furthermore, natural features such as valleys, ridges, and canyons can channel winds, accelerating fire spread or creating erratic fire behavior. Understanding these topographic influences is essential for predicting wildfire movement and planning effective suppression strategies (Rizza, Adlam, & Berger, 2022).

The fire behavior triangle highlights the critical role of fuel, weather, and topography in shaping wildfire dynamics. By understanding how these factors interact, we can better predict fire behavior and inform fire management strategies.

2.5 Fire Regime

A fire regime refers to the long-term pattern and characteristics of fire occurrence in a particular ecosystem or region. It is defined by several key variables, such as fire frequency, intensity, severity, seasonality, size, and type, which are shaped by the interaction between climate, vegetation (fuel), and ignition sources. Fire regimes provide a framework for describing how fires typically behave across space and time in different environments, enabling the classification of regions based on their historical fire activity and behavior (McLauchlan et al., 2020).

Building on this definition, figure 1.5 shows how fire processes unfold from the moment of ignition to the establishment of long-term patterns: These three conceptual triangles are not isolated; they are nested and interdependent. The fire triangle describes the basic conditions necessary for flame, which feed into the fire behavior triangle, governing spread and intensity. Over time and across space, recurrent fire behavior gives rise to distinctive fire regimes. Conversely, fire regimes influence fuel structures and landscape patterns, thereby feeding back into future fires' behavior and ignition potential. This nested, self-reinforcing relationship highlights the importance of viewing wildfires through a layered lens: from the chemistry of ignition at the micro level to the spatial dynamics of fire patterns across entire landscapes. Adopting such a multi-scale perspective is essential for understanding how wildfires emerge, evolve, and persist within complex socio-ecological systems.

[5] **The Northern Hemisphere** refers to the half of the Earth north of the Equator, including parts of Asia, Europe, North America, and the northern parts of Africa. **The Southern Hemisphere** lies to the south of the Equator, including regions such as Australia, South America, and southern parts of Africa.

Figure 1.5: Scaling of Fire Processes Across Space and Time

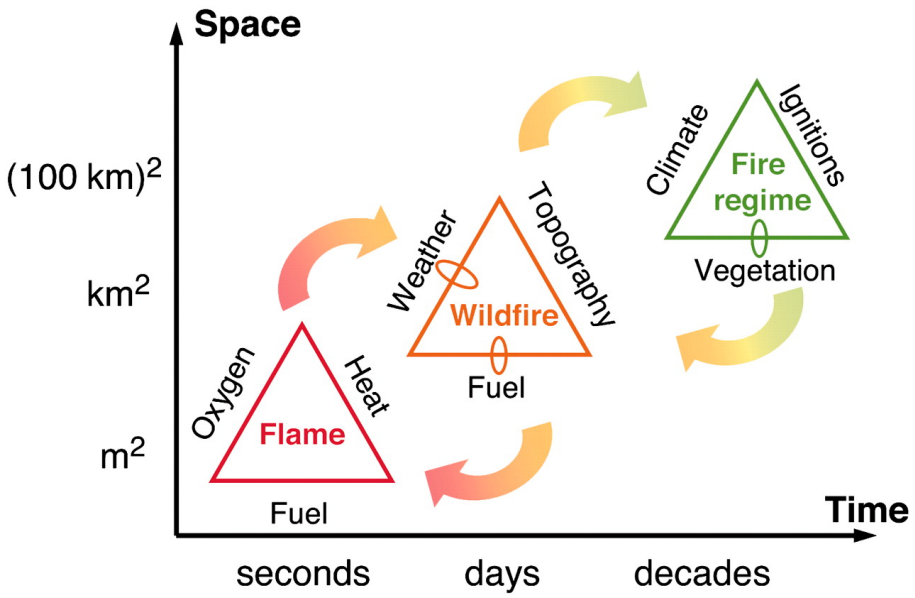

Source: (Moritz et al., 2005)

Fire regimes are fundamental to understanding ecosystem structure and function; they shape vegetation composition, influence species adaptations, and regulate nutrient cycling. Disruptions whether due to land use change or climate change, can lead to ecosystem transformations, fuel accumulation, and the emergence of novel fire dynamics. Therefore, reconstructing historical fire regimes and forecasting their potential shifts is essential for biodiversity conservation, ecological restoration, and fire risk mitigation (McLauchlan et al., 2020).

3 Impacts and Management of Wildfires

3.1 Wildfire Impacts

3.1.1 Ecological impacts

Although wildfires are often perceived solely as destructive forces, they can also play an important ecological role in certain fire-adapted ecosystems. Low-intensity fires can promote plant regeneration, maintain biodiversity, and prevent fuel accumulation, thereby reducing the risk of more severe fires. However, when fires become more frequent, more intense, or occur in ecosystems that are not fire-adapted, the consequences are largely detrimental (McLauchlan et al., 2020). Some notable effects are:

a) Vegetation Loss and Habitat Disruption

High-intensity wildfires consume tree canopies and understories, eliminating shelter and food for animal species and reducing native plant cover. This creates open ground where opportunistic or invasive plants can establish, further hindering the return of pre-fire communities (García-Redondo, Díaz-Raviña, & Regos, 2024).

b) Soil Degradation and Hydrological Alterations

Severe fires volatilize soil organic matter and kill key microbial communities while forming hydrophobic layers that repel water. This leads to increased runoff, as water flows over the surface rather than soaking into the soil, and erosion, where soil is carried away by wind or water. Together, these processes result in nutrient loss, hinder plant regrowth, and alter local water cycles (Farid et al., 2024).

c) Wildlife Displacement and Biodiversity Loss

Fire-driven habitat loss and resource scarcity cause direct mortality or force animals to relocate. Species with limited mobility or specialized niches are most at risk, and post-fire landscapes often favor invasive fauna, which can outcompete native fauna and contribute to a decline in local biodiversity (Smith, Huff, Hooper, Telfer, & Schreiner, 2000).

d) Altered Succession and Ecosystem Functioning

When high-severity fires recur too frequently, ecosystems can shift from forested to shrub- or grass-dominated states because trees cannot regrow fast enough between fires, allowing fire-adapted shrubs and grasses to take over. These state shifts diminish ecosystem resilience and disrupt key services such as carbon storage, since forests retain more carbon than shrublands or grasslands; nutrient cycling, as repeated burning and vegetation loss lead to soil degradation; and water regulation, as changes in vegetation alter surface runoff and water infiltration (McLauchlan et al., 2020).

3.1.2 Environmental Impacts

Wildfires not only reshape ecosystems but also drive substantial changes in atmospheric composition, air quality, and water cycles, creating both immediate and long-term environmental consequences.

a) GHG Emissions and the Climate–Fire Loop

Greenhouse gases (GHGs) like carbon dioxide (CO_2), methane (CH_4), and nitrogen oxides (NO_x) are essential for maintaining Earth's habitable temperature by trapping heat in the atmosphere, a process known as the greenhouse effect. However, this effect intensifies when their concentrations become excessive, driving global warming. Wildfires act as both a source and a consequence of elevated GHG concentrations. On one hand, they emit vast amounts of CO_2, around 5 to 8 billion tonnes annually (Samborska & Ritchie, 2024) . On the other hand, their frequency and severity are increasing under hotter, drier conditions, forming a reinforcing feedback loop (figure 1.6) in which fires accelerate warming, and warming amplifies fire-prone conditions (Singh, 2022).

b) Air Quality Deterioration

In addition to greenhouse gas emissions, wildfires release large quantities of air pollutants[6] that severely degrade atmospheric quality. These include fine particulate matter ($PM_{2.5}$), carbon monoxide (CO), nitrogen oxides (NO_x), and volatile organic compounds (VOCs), all of which contribute to smog formation and elevated ground-level ozone[7]. Such pollutants can travel hundreds or even thousands of

[6] **$PM_{2.5}$**, **CO**, **NO_x**, and **VOCs** are all air pollutants released during combustion.
[7] **Smog** is a type of air pollution primarily composed of **ground-level ozone**, which is a harmful gas formed when NO_x and VOCs react in the presence of sunlight.

Figure 1.6: Fire and Climate Feedback Loop

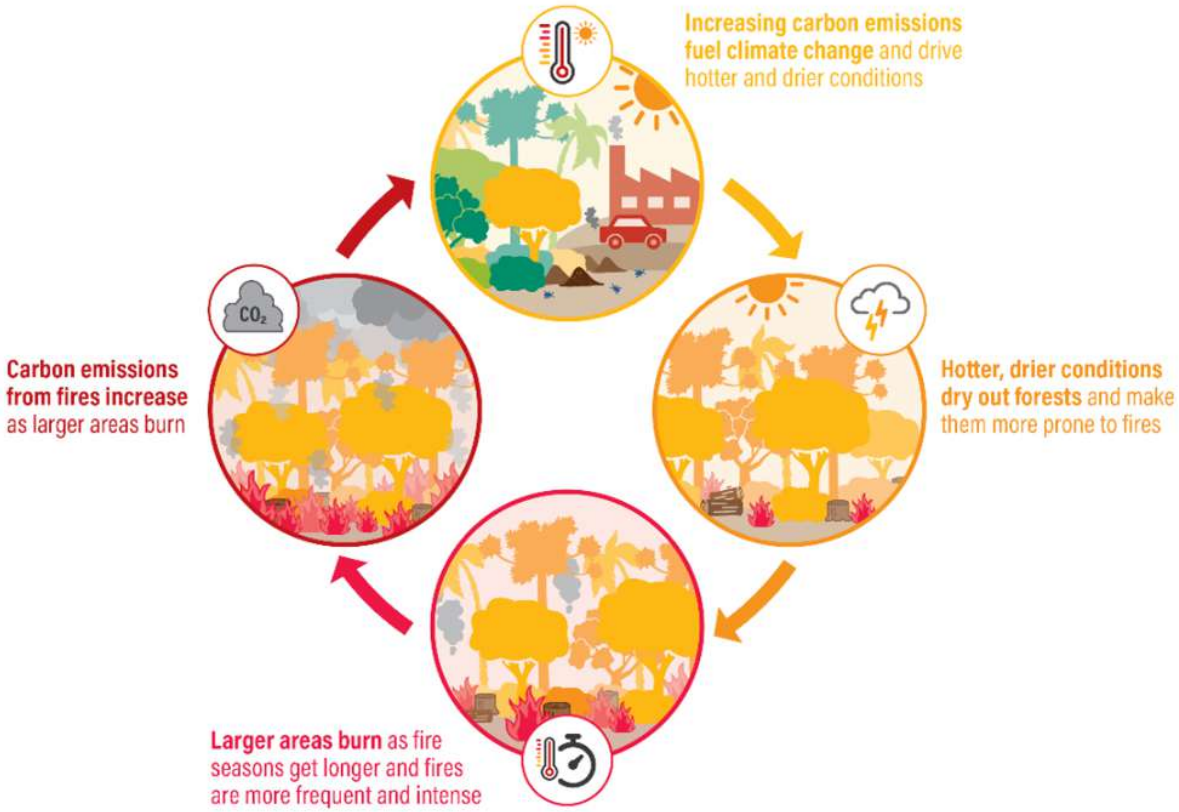

Source: World Resources Institute Retrieved April 10

kilometers from the fire's origin, leading to regional-scale declines in air quality. Also, prolonged smoke exposure can alter atmospheric chemistry, reduce visibility, and affect weather patterns by interacting with solar radiation and cloud formation (R. Xu et al., 2020).

3.1.3 Human Health Impacts

a) Vulnerable Populations

The health effects of wildfire smoke are not experienced equally across the population. Children and older adults are more vulnerable due to developing or aging respiratory systems, while pregnant individuals face increased risks of adverse birth outcomes when exposed to elevated air pollution. Outdoor workers, particularly those in agriculture or firefighting, are at higher risk due to prolonged and repeated exposure to smoke under physically demanding conditions. These cumulative risks are amplified in populations with limited access to health care, protective equipment, or early warning systems (R. Xu et al., 2020).

b) Short-Term Health Risks

Wildfire smoke contains high concentrations of air pollutants that pose immediate risks to human health. Short-term exposure is strongly associated with respiratory symptoms such as coughing, wheez-

ing, shortness of breath, and eye and throat irritation. These symptoms are frequently accompanied by increased emergency department visits and hospitalizations for asthma, bronchitis, chronic obstructive pulmonary disease (COPD), and respiratory infections. During major wildfire events, $PM_{2.5}$ levels have been recorded at concentrations exceeding $500\mu g/m^3$, far above international safety thresholds, coinciding with 10% to 30% surges in respiratory-related hospital admissions in affected areas (R. Xu et al., 2020).

Figure 1.7: Annual Global PM2.5 Emissions from Wildfires

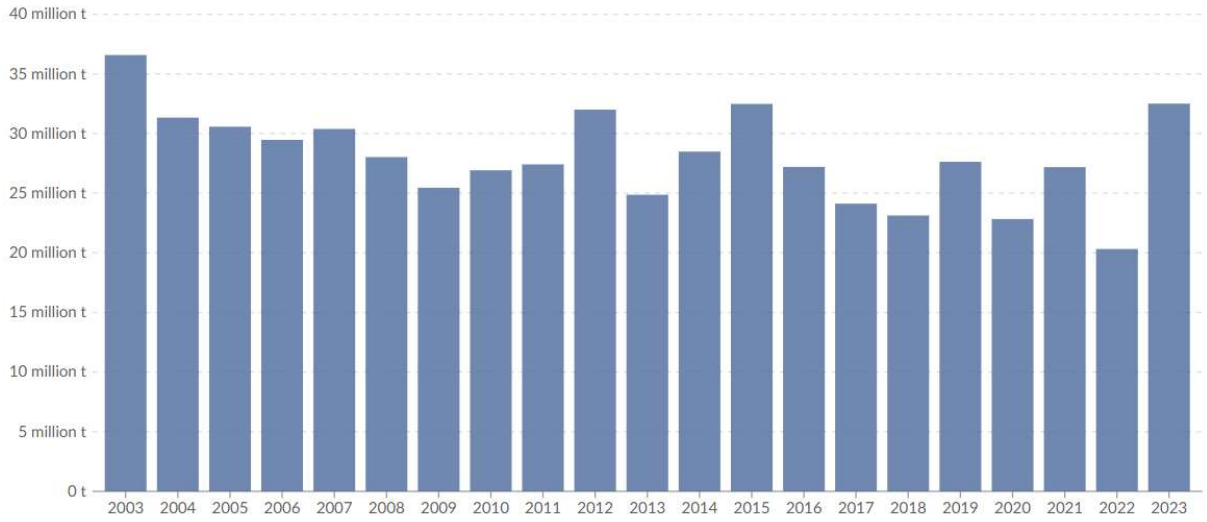

Source: Our World in Data Retrieved April 13

As illustrated in Figure 1.7, global emissions of fine particulate matter ($PM_{2.5}$) from wildfires have exhibited marked annual variability, consistently exceeding 20 million tonnes. This underscores the scale of pollutant exposure during fire seasons and the associated short-term health burden. Over time, such recurrent exposure may contribute to more persistent and systemic health effects.

c) Long-Term Exposure Effects

Repeated or prolonged exposure to wildfire smoke may lead to chronic health effects. Studies have documented persistent declines in lung function and respiratory symptoms lasting months after exposure. Longitudinal research also links extended smoke exposure to elevated cardiovascular risk, including increased blood pressure and inflammation. Affected individuals frequently report poorer overall health and higher healthcare use than those not exposed (R. Xu et al., 2020).

d) Mental Health Effects

The psychological consequences of wildfires frequently persist beyond the initial emergency phase, affecting mental health through displacement, property loss, and exposure to trauma. Reported outcomes include increased rates of anxiety, depression, post-traumatic stress disorder (PTSD), and sleep disturbances, particularly among those who experience evacuation or direct threats to life. In children, exposure to wildfire events has been associated with emotional distress, behavioral issues, and reduced academic performance that can last for years. The mental health burden is amplified in communities with repeated wildfire events and inadequate recovery support (R. Xu et al., 2020).

3.1.4 Economic Impacts

a) Direct Costs

Wildfires impose substantial direct costs on governments, businesses, and households. These costs include fire suppression efforts, emergency response operations, and damage to infrastructure, homes, and commercial properties. In the United States, suppression spending has more than tripled since the late 1980s, reflecting the growing frequency and severity of wildfires, particularly on federally managed lands (Office, 2022). Beyond North America, the economic burden is also significant; in Southern Europe, annual production losses due to wildfires are estimated at EUR 13 to EUR 21 billion (Meier, Elliott, & Strobl, 2023).

b) Indirect Costs

Beyond immediate damages, wildfires generate significant indirect costs through business interruption, lost tourism revenue, and disrupted supply chains. For example, Australia's 2019–2020 "Black Summer" bushfires caused over AUD 2.8 billion in losses to the tourism industry, driven by travel cancellations, smoke-related air quality issues, and park closures (Reiner, Pathirana, Sun, Lenzen, & Malik, 2024). Wildfires can also negatively affect labor markets; they have been linked to short-term declines in employment growth in affected regions (Office, 2022).

c) Long-Term Impacts

The economic burden of wildfires extends long after the flames are extinguished. Long-term impacts include rising insurance premiums, depreciation of land and property values, and increased public health expenditures due to smoke-related illnesses. According to the (U.S. Joint Economic Committee, 2023), Wildfires cost the United States economy between USD 394 billion and USD 893 billion annually, equivalent to 2 – 4% of national GDP when accounting for direct, indirect, and long-term damages .

d) Wildfires' Uneven Economic Burden

The economic impacts of wildfires are not distributed equally. Low-income households and rural communities often face greater challenges in recovering from fire-related losses due to lower insurance coverage, limited access to financial resources, and dependency on climate-sensitive sectors such as agriculture and tourism. These groups may suffer prolonged financial hardship, widening existing socioeconomic disparities, particularly in regions with repeated fire exposure or inadequate recovery support(U.S. Joint Economic Committee, 2023).

The diverse and far-reaching impacts of wildfires underscore the vulnerability of ecosystems, human health, and the economy. The severity of these consequences emphasizes the need for urgent action to address both the immediate and long-term effects of wildfires. Recognizing these challenges is essential for building resilience and ensuring sustainable approaches to managing wildfire risks in the future.

3.2 Fighting Fire: Prevention, Mitigation and Management and Strategies.

As wildfires grow more frequent and severe across the globe, responding to this threat requires a broad set of actions that extend beyond extinguishing flames. These include both proactive measures

to reduce risk and reactive, coordinated efforts that integrate scientific knowledge, public policy, and operational practices. As climate pressures intensify and human presence expands in fire-prone areas, such coordination has become essential for managing increasingly complex fire regimes and fostering long-term resilience (Chuvieco et al., 2023).

3.2.1 Prevention And Mitigation

Wildfire prevention and mitigation refer to the set of measures aimed at reducing both the likelihood of fire ignition and the potential severity of wildfires when they occur, especially in areas with elevated risk due to natural or anthropogenic factors. As defined by the Food and Agriculture Organization (Food & Organization, 2007), these measures encompass all actions intended to avoid wildfire outbreaks or to limit the environmental and social conditions that favor ignition.

a) Fuel Management

Fuel management is one of the most widely applied strategies in wildfire prevention and mitigation. It involves manipulating vegetation to reduce fuel loads or disrupt fuel continuity, typically through practices such as prescribed burning, mechanical thinning, and biomass removal. When implemented under appropriate ecological and climatic conditions, these interventions can significantly reduce the likelihood of ignition, attenuate fire intensity, and limit flame spread, particularly under moderate weather conditions. However, their effectiveness is influenced by factors like type of treatment, and the frequency of application (Oliveras Menor et al., 2025).

b) Public Education and Community Engagement

Human activity remains the leading cause of wildfire ignitions in many parts of the world. Consequently, prevention strategies must prioritize public awareness and promote safer behaviors. Educational campaigns, community workshops, and local fire prevention programs are vital tools for encouraging risk-reducing practices, such as refraining from open burning during periods of elevated fire danger. The scale of population exposure underscores the urgency of such efforts: in the United States alone, approximately 115 million people, more than one-third of the population, reside in high wildfire risk counties[8]. Community-based programs increase awareness, preparedness, and play a key role in decreasing the number of human-induced fire ignitions over time (Food & Organization, 2024).

c) Land Use Planning and Infrastructure Regulation

Strategic land-use planning reduces ignition risks by controlling where and how development occurs in fire-prone zones. As illustrated in figure 1.8, policies such as limiting expansion into wildland areas and mandating fire-resistant construction materials help lower the chances of fire ignition and reduce potential damage. Residential areas in the wildland–urban interface (WUI)[9] with widely spaced homes surrounded by flammable vegetation face higher wildfire risks, thus thoughtful spatial planning is essential for reducing ignition likelihood (Syphard, Keeley, Massada, Brennan, & Radeloff, 2012).

[8] Wildfire Risk to Communities Retrieved April 20

[9] The **WUI** refers to the area where human development, such as homes and businesses, intersects with undeveloped wildland.

Figure 1.8: Land Use Planning strategies

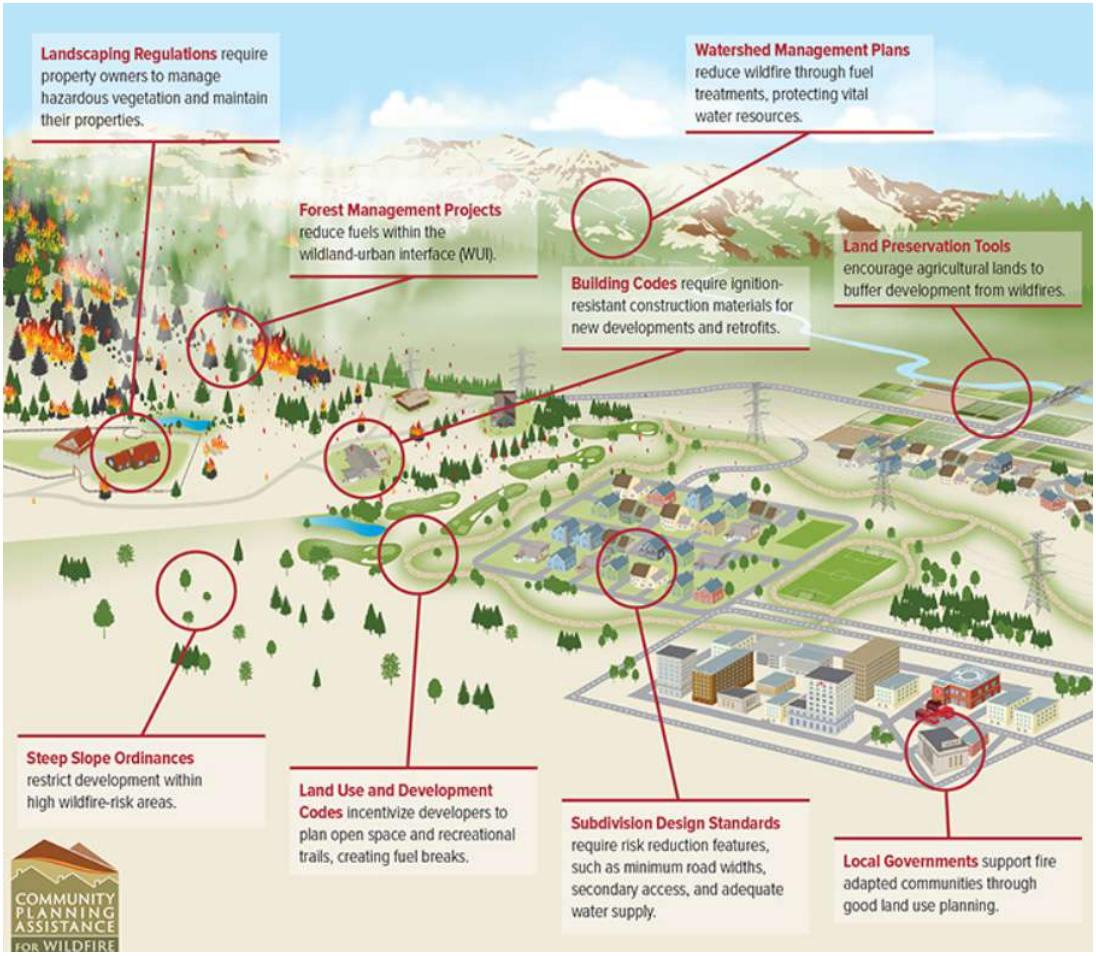

Source: Wildfire Risk to Communities Retreived April 20

d) Early Warning Systems and Fire Weather Monitoring

Technological tools play an essential role in wildfire prevention by enabling real-time risk assessments and supporting decision-making during periods of elevated fire danger. Remote sensing, meteorological forecasting, and fire danger rating systems, such as the Canadian Fire Weather Index and the U.S. National Fire Danger Rating System, help authorities identify where and when ignition is most likely to occur. These forecasts provide the basis for enforcing temporary restrictions on high-risk activities, including agricultural burning and the use of machinery in vulnerable landscapes. By offering more timely and spatially precise insights, such systems have become integral to modern prevention strategies (Food & Organization, 2024).

e) Climate Change Mitigation

Limiting global temperature rise requires effective reductions in greenhouse gas emissions and is crucial for reducing future wildfire risks. By curbing emissions, it is possible to significantly reduce the frequency and intensity of wildfires, which are projected to escalate under current high-emission scenarios (R. Xu et al., 2020). In parallel, adaptive land and forest management strategies, such as promoting

species resilience, maintaining ecosystem integrity, and conserving carbon-rich landscapes, can buffer ecosystems against the effects of climate change while also reducing fire susceptibility (Moritz et al., 2014).

3.2.2 Management

Wildfire management encompasses the organized efforts to detect, respond to, and suppress active fires. It plays a critical role in fire-prone regions near human settlements, biodiversity reserves, or vulnerable infrastructure, where rapid intervention is essential to minimize harm (Food & Organization, 2024).

a) Operational Preparedness and Detection Systems

Preparedness and detection form the foundation for timely and effective response. Preparedness involves maintaining trained firefighters, ensuring equipment is operational, and establishing clear response protocols. Strategic resource placement, along with continuous capacity-building, such as simulation drills and scenario-based exercises helps maintain readiness during critical fire seasons (Food & Organization, 2024).

Detection systems have also advanced considerably. While fire observation once relied on watchtowers and community reporting, modern approaches now include satellite imagery, drone surveillance, and automated camera networks capable of identifying heat and smoke in real time. When integrated into centralized platforms, these technologies enable faster detection, quicker response times, and more coordinated deployment of firefighting resources (Sairi, Labed, & Miles, 2024).

b) Suppression Strategies and Tactical Decision-Making

Once a wildfire is detected, suppression efforts aim to contain or extinguish it while minimizing risks to personnel and communities. Fire managers assess fire behavior, fuel conditions, topography, and meteorological forecasts to determine appropriate tactics. Direct suppression typically involves constructing firelines and applying water or retardants near the fire perimeter, while indirect approaches, such as backburning or aerial suppression, are used in complex terrain or during high-intensity events.

Modern suppression strategies are increasingly data-driven. Tools such as GIS (Geographic Information Systems), predictive fire modeling, and field reports help fire managers make informed decisions. Moreover, artificial intelligence (AI) and machine learning (ML) are being incorporated into wildfire management. These technologies can forecast fire spread, optimize resource allocation, and enhance situational awareness, improving the effectiveness and safety of firefighting operations (Martell, 2015).

c) Interagency Coordination and Resource Management

Effective wildfire management requires coordinated efforts across various agencies and jurisdictions. Standardized frameworks such as the Incident Command System (ICS) help define roles, streamline communication, and manage resources efficiently during emergencies[10]. In Europe, the European Forest Fire Information System (EFFIS) serves as a critical platform for harmonizing wildfire data and coordinating responses among member states. EFFIS provides near real-time information on fire occurrences,

[10] Incident Command System Retreived April 22

supports the assessment of fire danger levels, and aids in the allocation of resources across borders (San-Miguel-Ayanz et al., 2024). Such systems illustrate the importance of integrated approaches in managing wildfires, especially in regions where fires can transcend national boundaries.

d) Post-Fire Recovery and Adaptive Management

The end of active burning marks the beginning of post-fire recovery, which is critical to reduce long-term impacts and prevent secondary disasters such as erosion, landslides, or invasive species spread. Restoration efforts may include reforestation, soil stabilization, and habitat rehabilitation, as well as rebuilding infrastructure and assisting displaced communities. Post-fire analysis plays a key role in adaptive management by assessing fire behavior, suppression effectiveness, and ecosystem response to support learning and continuous improvement in wildfire strategies. This is essential for developing resilience under changing fire regimes and climate conditions (Huidobro et al., 2024).

A comprehensive fire governance approach is most effective when it moves beyond isolated actions and embraces a connected strategy that spans early risk reduction, strategic response during crises, and long-term ecological and social restoration. Such an approach lays the groundwork for more sustainable coexistence with fire in a rapidly changing world.

4 Global Wildfires: Trends, and Regional Insights

In recent decades, the duration and severity of fire weather seasons have increased globally, primarily due to anthropogenic climate change. From 1979 to 2013, fire weather seasons expanded across nearly 29.6 million km² (25.3%) of the Earth's vegetated regions, resulting in an 18.7% increase in the global average fire weather season length, roughly equivalent to one month [11]. Furthermore, the area experiencing prolonged fire weather conditions has more than doubled, significantly expanding environments conducive to wildfires (Jolly et al., 2015).

Reflecting these global patterns, regional analyses also reveal significant trends. In the United States, wildfire seasons have extended by approximately 17%, with individual fires growing in size by 78% and their frequency rising by 12% (Cattau, Wessman, Mahood, & Balch, 2020). In Australia, the number of extreme fire weather days increased by 56%, and the national fire season has lengthened by approximately 27 days, marking a 20% rise between 1979 and 2019[12]. Similarly, in the Mediterranean Basin, which is characterized by hot and dry summers, regions like Portugal have experienced fire activity beginning 23 to 50 days earlier than historical norms (Silva, Carmo, Rio, & Novo, 2023).

Recent data indicate that global temperatures have already risen by 1.3°C relative to pre-industrial levels (1850–1900) (Organization, 2025). If current warming trends continue, the frequency of wildfires is projected to increase significantly, impacting more than 74% of the Earth's land area by the century's end. However, if immediate mitigation measures are implemented to limit the global temperature rise to 2.0°C or 1.5°C above pre-industrial levels, up to 60% or 80% of the projected increase in wildfire exposure, respectively, could be prevented (R. Xu et al., 2020).

Although climate change is the primary driver, other human-induced factors also contribute to shifting wildfire regimes. In particular, land-use changes, such as rural abandonment and fire suppression

[11] Headwaters Economics Retrieved April 25
[12] CSIRO Retrieved April 25

policies, have increased landscape flammability by enabling fuel accumulation and altering vegetation structures (Pausas & Keeley, 2021). Together with climate change, these factors are amplifying wildfire risks across regions.

Conclusion

This chapter has provided a comprehensive overview of the fundamental mechanisms and impacts of wildfires, establishing a solid conceptual foundation for the remainder of this dissertation. It began by defining wildfires as complex socio-ecological hazards driven by both natural and anthropogenic factors. Key concepts such as the fire triangle, fire behavior triangle, and fire regimes were introduced to explain how fires ignite, propagate, and persist across landscapes over time.

Building on these foundational concepts, the chapter examined the multifaceted ecological, environmental, health, and economic impacts of wildfires, and underscored their destructive potential in both natural and human systems. It also explored global patterns and emerging trends—such as the intensification of fire seasons, increased ignition frequency, and growing fire sizes—which are being exacerbated by climate change and shifting land-use practices. These developments highlight the urgent need for improved prevention, forecasting, and long-term fire management strategies across diverse regions.

Furthermore, the discussion emphasized that wildfires are not solely natural phenomenabut also phenomena deeply shaped by broader social, environmental, and land-use dynamics. Modern fire management must therefore adopt an integrated approach that spans prevention, mitigation, suppression, and post-fire recovery. Contemporary strategies, including fuel management, land-use planning, early warning systems, and the incorporation of climate change mitigation, were presented as critical components of this broader fire governance framework.

Understanding the scientific underpinnings of wildfire behavior and its impacts is therefore essential for developing predictive tools capable of informing policy and operational decisions. The insights developed in this chapter set the stage for the exploration of artificial intelligence techniques in the following sections. By combining domain knowledge with advanced predictive models, the aim is to enhance wildfire risk assessment and provide actionable insights to support proactive, data-informed decision-making in fire-prone landscapes worldwide.

CHAPTER 2:

Artificial Intelligence Concepts for Predictive Modeling

Chapter 2

Artificial Intelligence Concepts for Predictive Modeling

Introduction

Predicting wildfire occurrence presents unique challenges due to the complex interactions between climatic, environmental, and anthropogenic factors. To model such dynamics effectively, modern data-driven approaches increasingly rely on artificial intelligence (AI), particularly machine learning (ML) and deep learning (DL) techniques. This chapter establishes the theoretical foundations that underpin the modeling framework presented in Chapter 3. It begins by introducing key ML concepts, followed by a focused discussion on deep learning models, including artificial neural networks and recurrent architectures. The chapter concludes with an overview of explainable artificial intelligence (XAI), presenting two interpretability techniques used in this work for building a trustworthy and transparent wildfire prediction model.

1 Introduction to Machine Learning

1.1 Definition of AI and Machine Learning

Artificial Intelligence (AI) encompasses computational methods that enable machines to perform tasks typically requiring human intelligence, such as reasoning, perception, and decision-making. As defined by Chollet, Kalinowski, and Allaire (2022), "AI can be described as the effort to automate intellectual tasks normally performed by humans." Within this broad domain, Machine Learning (ML) has emerged as a central subfield, closely related to mathematical statistics, that focuses on systems capable of learning from data rather than relying on explicitly programmed rules, like traditional programming.

Figure 2.1: Rule-Based Programming vs ML

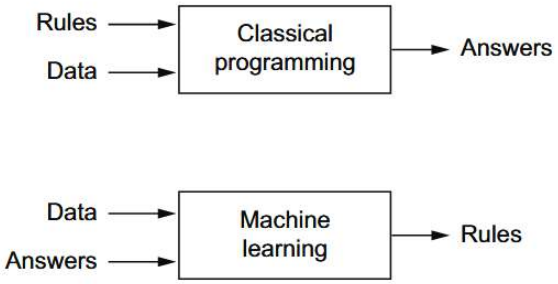

Source: (Chollet et al., 2022)

Instead of being given a fixed set of instructions, a machine learning system is trained using many examples related to a specific task. By analyzing these examples and their corresponding outcomes, it learns patterns in the data and develops its own rules for making predictions or decisions automatically.

1.2 Types of Machine Learning

Machine Learning Algorithms are generally divided into three main types: Supervised Learning, Unsupervised Learning, and Reinforcement Learning (Figure 2.2). While these categories cover most use cases, other, more specialized types also exist.

1.2.1 Supervised Learning

Supervised learning represents the most widely used category of machine learning. It relies on the availability of a dataset in which each instance consists of input variables $x^{(1)}, \ldots, x^{(N)}$ and an associated known output $y^{(1)}, \ldots, y^{(N)}$. These labeled examples (training data) serve as the foundation for training, where the goal is to learn a mapping function f that captures the relationship between inputs and outputs. This learned function can then be used to make predictions on unseen data (testing data) (Lemberger, Batty, Morel, & Raffaëlli, 2015).

Supervised learning tasks can be broadly divided into two main categories:

- **Regression:** The aim is to predict continuous numerical values. Example applications include temperature forecasting, stock price prediction, or estimating burned area in wildfire events.
- **Classification:** The objective is to assign instances to predefined classes. This includes problems like email spam detection, image recognition, or predicting fire occurrence as a binary outcome.

Figure 2.2: Machine Learning Types

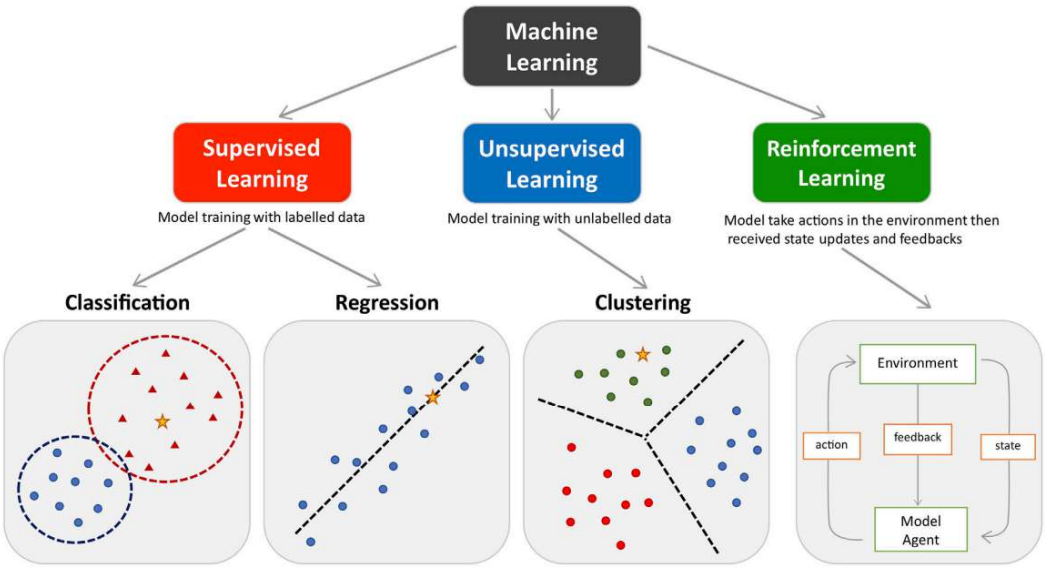

Source: (Peng et al., 2021)

To address these tasks, a wide variety of supervised learning algorithms have been developed. These algorithms can be grouped into the following categories based on their underlying methodological principles:

⟶ **Linear Models:** Linear Regression for regression tasks and Logistic Regression for classification.

⟶ **Instance-Based Learning:** *k*-Nearest Neighbors, which makes predictions based on similarity to training examples.

⟶ **Kernel-Based Methods:** Support Vector Machines (SVM), effective for both linear and non-linear classification problems.

⟶ **Tree-Based Methods:** Decision Trees, Random Forests, and Gradient Boosting Machines (e.g., XGBoost), which are versatile and interpretable models used in both regression and classification.

⟶ **Neural Network Models:** Including both shallow and deep architectures, suitable for capturing complex patterns across a variety of supervised learning tasks.

1.2.2 Unsupervised Learning

Unsupervised learning operates without prior labeling of the training data. The primary objective is for the system to autonomously identify structure within the data by grouping similar examples into meaningful categories or clusters. This typically relies on a measure of distance or similarity between observations to guide the grouping process. However, interpreting the resulting groupings, such as understanding what each cluster represents, remains a task that depends on human expertise and domain knowledge (Lemberger et al., 2015)

Unsupervised learning encompasses two primary tasks:

- **Clustering:** The goal is to group data points into clusters based on similarity. Common algorithms include:

  $\longrightarrow$ k-Means Clustering

  $\longrightarrow$ Hierarchical Clustering

- **Dimensionality Reduction:** This involves projecting high-dimensional data into lower-dimensional spaces while preserving important structure. It is useful for visualization or as a preprocessing step. Techniques include:

  $\longrightarrow$ Principal Component Analysis (PCA)

  $\longrightarrow$ t-Distributed Stochastic Neighbor Embedding (t-SNE)

  $\longrightarrow$ Uniform Manifold Approximation and Projection (UMAP)

1.2.3 Reinforcement Learning

Reinforcement learning is a type of machine learning in which a model learns to interact with an environment by receiving feedback in the form of rewards or penalties. The model performs actions within the environment and uses the resulting feedback to adjust its future behavior. The goal is to maximize cumulative reward over time by learning which actions lead to the most favorable outcomes. Unlike supervised learning, reinforcement learning does not require labeled examples; instead, it relies on trial-and-error to identify optimal strategies. Reinforcement learning is widely used in robotics, gaming, and other applications where a system must learn to operate in complex environments and make decisions based on its observations (Sutton & Barto, 2015).

1.3 Machine Learning Pipeline

1.3.1 Data Collection and Exploratory Data Analysis (EDA)

The process begins with gathering data from various sources and formats, ranging from structured tables to unstructured records. Exploratory Data Analysis (EDA) is then conducted to understand data distributions, detect patterns or anomalies, and examine relationships between variables. Insights from EDA inform decisions about variable transformation, outlier treatment, and data quality improvement before modeling.

1.3.2 Data Cleaning and Missing Value Handling

Real-world data often contains missing values, duplicates, or inconsistent formats that must be addressed. Common strategies include deletion, imputation (mean, mode, or model-based), and other approaches to ensure dataset consistency and reliability

1.3.3 Feature Engineering and Selection

Feature engineering involves creating or transforming variables to better capture relevant patterns for the learning task. This may include deriving new features, encoding categorical data, normalizing continuous variables, or applying domain-specific transformations. Feature selection helps reduce dimensionality, minimize noise and overfitting risks, and improve computational efficiency.

1.3.4 Data Splitting

To evaluate model generalization, the dataset is split into training, validation, and test sets. Cross-validation techniques are commonly used to assess model stability and guide hyperparameter tuning. Crucially, the test set remains untouched during model development to prevent information leakage and biased performance estimates.

1.3.5 Model Training and Hyperparameter Tuning

A suitable learning algorithm is chosen based on the problem and the data. The model is trained to identify meaningful patterns for accurate predictions on new data. Simultaneously, hyperparameters are tuned using the validation set to enhance generalization. Together, these steps shape the model's ultimate performance.

1.3.6 Model Evaluation and Deployment

Once trained, the model is tested on new data to assess its performance. Depending on the task, different metrics are used, with the choice also influenced by data characteristics; for instance, some are more informative in cases like imbalanced datasets. If the performance is satisfactory, the model is deployed into real-world systems, where it is monitored and updated as needed to maintain reliability (Kampezidou, Tikayat Ray, Bhat, Pinon Fischer, & Mavris, 2024).

1.4 Evaluation Metrics for Binary Classification

In binary classification tasks, the objective is to assign instances to one of two classes, commonly referred to as the positive and negative class. Assessing the performance of such classifiers requires metrics that capture different aspects of correctness, error, and trade-offs between types of predictions. This section outlines the most commonly used evaluation metrics.

1.4.1 Confusion Matrix

A confusion matrix is a tabular representation of the model's predictions versus the actual class labels.

Figure 2.3: 2x2 Confusion Matrix

		Actual Class	
		Positive (**P**)	Negative (**N**)
Predicted Class	Positive (**P**)	True Positive (**TP**)	False Positive (**FP**)
	Negative (**N**)	False Negative (**FN**)	True Negative (**TN**)

Source: The Science of Machine Learning & AI Retreived on May 24th

It consists of four components:

- **True Positives (TP)**: Instances correctly predicted as positive.

- **False Positives (FP)**: Instances incorrectly predicted as positive.
- **True Negatives (TN)**: Instances correctly predicted as negative.
- **False Negatives (FN)**: Instances incorrectly predicted as negative.

These quantities form the basis for most other evaluation metrics.

1.4.2 Accuracy

Accuracy is the proportion of correctly classified instances over the total number of instances:

$$\textbf{Accuracy} = \frac{TP + TN}{TP + FP + TN + FN} \tag{2.1}$$

While simple and intuitive, accuracy can be misleading in imbalanced datasets, where one class is much more frequent than the other.

1.4.3 Precision

Precision measures the proportion of positive predictions that are actually correct:

$$\textbf{Precision} = \frac{TP}{TP + FP} \tag{2.2}$$

It reflects the reliability of positive predictions and is particularly important when false positives are costly.

1.4.4 Recall (Sensitivity or True Positive Rate)

Recall quantifies the proportion of actual positives that are correctly identified:

$$\textbf{Recall} = \frac{TP}{TP + FN} \tag{2.3}$$

High recall indicates that the model is effective at detecting positive instances, though potentially at the expense of precision.

1.4.5 F1 Score

The F1 score is the harmonic mean of precision and recall, providing a single metric that balances both:

$$\textbf{F1 Score} = 2 \cdot \frac{\textbf{Precision} \cdot \textbf{Recall}}{\textbf{Precision} + \textbf{Recall}} \tag{2.4}$$

It is especially useful when there is an uneven class distribution and both false positives and false negatives are important.

1.4.6 ROC and Precision-Recall Curves

Evaluating probabilistic classifiers requires metrics that consider the model's performance across all classification thresholds. Two commonly used tools are the Receiver Operating Characteristic (ROC) curve and the Precision-Recall (PR) curve, each emphasizing different aspects of model behavior.

ROC Curve and AUC.

The ROC curve plots the True Positive Rate (TPR, or Recall) against the False Positive Rate (FPR) as the classification threshold varies. The Area Under the ROC Curve (AUC) provides a scalar measure of separability between classes:

- **AUC = 1.0** indicates perfect class separation.
- **AUC = 0.5** corresponds to performance equivalent to random guessing.

The ROC curve offers an intuitive view of the trade-off between sensitivity and the false positive rate. However, in imbalanced datasets, it may overestimate performance by giving undue weight to the abundant negative class.

Precision-Recall Curve and AUPRC.

The PR curve plots Precision versus Recall across classification thresholds, focusing exclusively on the positive class. The Area Under the Precision-Recall Curve (AUPRC) provides a summary of how well the model identifies true positives without being misled by the abundance of true negatives.

Unlike ROC-AUC, the AUPRC offers a clearer picture of model performance when the positive class is rare (Saito & Rehmsmeier, 2015). It is therefore the preferred evaluation tool in imbalanced classification settings like our case.

1.5 Challenges in Machine Learning

1.5.1 Underfitting and Overfitting

A key challenge in supervised learning is ensuring that models generalize well to unseen data. Two major issues that hinder this are underfitting and overfitting. Underfitting happens when a model is too simple to capture the underlying patterns in the data, resulting in poor predictive performance on both training and test sets. Conversely, overfitting occurs when a model is overly complex and begins to memorize the training data, including random fluctuations or irrelevant noise. This leads to excellent performance on training data but poor accuracy on new, unseen samples. These phenomena are related to the bias–variance trade-off, a fundamental concept describing the balance between a model's ability to minimize errors on training data (low bias) and its sensitivity to small fluctuations within that data (low variance). Achieving an optimal balance between bias and variance is crucial for building models that generalize effectively beyond the training dataset (Sohil, Sohali, & Shabbir, 2022).

1.5.2 Data Leakage

Data leakage refers to the unintended use of information in the training process that would not be available when making predictions on new data. This results in inflated model performance during evaluation but poor generalization to unseen data. Leakage can occur when features directly or indirectly contain target information, or when data preprocessing is improperly applied before data splitting. Preventing data leakage requires careful separation of training and test datasets and ensuring that no future or target-related information influences the training phase (Apicella, Isgrò, & Prevete, 2024).

1.5.3 Imbalanced Datasets

A common challenge in classification tasks is the presence of imbalanced datasets, where one class is significantly underrepresented compared to the other. This imbalance can lead machine learning models to become biased toward the majority class, since minimizing prediction error during training often results in favoring the dominant class. In such cases, the model may overlook or poorly capture the patterns associated with the minority class, which is often the class of greater interest. Addressing class imbalance is critical to ensure that the model learns meaningful distinctions between all categories rather than defaulting to the majority (Haibo He & Garcia, 2009).

2 Introduction to Deep Learning

2.1 Definition of Deep Learning

Deep learning (DL) is a subfield of machine learning that has gained a lot of attention recently. It relies on computational models composed of multiple layers of processing, known as *artificial neural networks*. These models learn data representations or transformations through a hierarchy of layers, where each successive layer captures increasingly abstract and meaningful patterns (LeCun, Bengio, & Hinton, 2015).

What makes deep learning distinctive is its ability to automatically discover complex structures in datasets. Unlike traditional ML approaches that often depend on manually designed features, DL models can learn directly from raw inputs, adjusting their internal representations through training. This capacity allows deep learning to tackle tasks involving high-dimensional, unstructured data such as images, audio, and text with remarkable performance (Chollet et al., 2022).

However, this strength also comes with a prerequisite: deep learning models require substantial amounts of data to fully realize their potential, as they need enough examples to extract complex patterns and to ensure that the learned representations generalize well to new, unseen data. Therefore, DL models tend to perform better with more data, unlike ML models, which often plateaus after a certain point.

Figure 2.4: DL vs ML

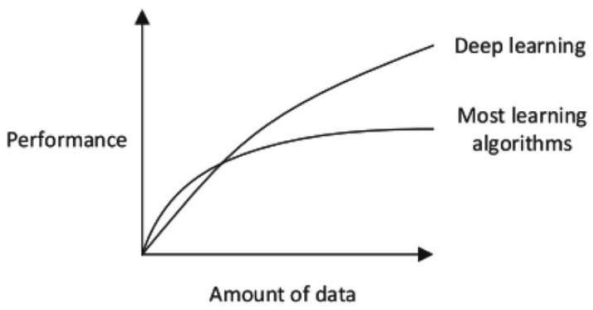

Source: (Sarker, 2021)

2.2 Artificial Neural Networks

Artificial neural networks are at the core of deep learning algorithms. A typical neural network is primarily composed of many simple, interconnected processing units called neurons.

2.2.1 Structure of Neurons

Artificial neurons were developed in part by drawing inspiration from our understanding of the brain (Chollet et al., 2022). In a biological neuron (figure 2.5a), dendrites receive signals, which are processed in the cell body and transmitted through the axon to other neurons. Similarly, an artificial neuron (figure 2.5b) is a computational unit that receives inputs, processes them, and produces an output.

Figure 2.5: Structural Analogy Between a Biological Neuron and an Artificial Neuron

(a) Biological Neuron

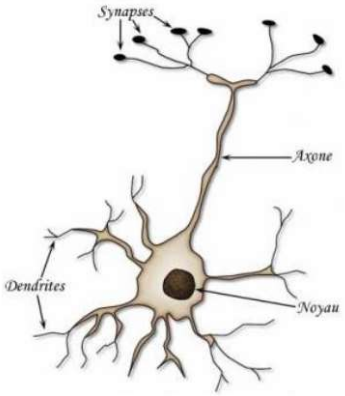

Source: (Chekroun, 2009)

(b) Artificial Neuron

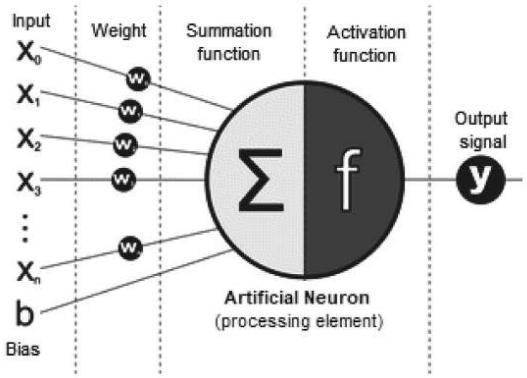

Source: (Sarker, 2021)

At its core, an artificial neuron takes a set of input values, multiplies each by an associated weight, adds a bias term, and computes a weighted sum. This weighted sum is then passed through a non-linear activation function to produce the neuron's output. Mathematically, this process can be described as:

$$z = \sum_{i=1}^{n} w_i x_i + b \quad \text{and} \quad y = \phi(z) \tag{2.5}$$

where:

- x_i are the input features,
- w_i are the corresponding weights,
- b is the bias term,
- ϕ is the activation function,
- y is the output of the neuron.

2.2.2 Activation Functions

To enable neural networks to learn complex, non-linear relationships, a non-linear transformation must be applied after the linear combination of inputs. This role is fulfilled by the activation function

which introduces non-linearity into the network. Without it, even a deep neural network would behave like a linear model (Nwankpa, Ijomah, Gachagan, & Marshall, 2018).

Several activation functions are commonly used in practice, each with distinct properties:

a) Sigmoid Function

The sigmoid activation function squashes input values into the range $(0, 1)$ and is defined as:

$$\textbf{Sigmoid}(z) = \frac{1}{1 + e^{-z}} \tag{2.6}$$

It is often used when the output needs to represent a probability.

b) Hyperbolic Tangent (Tanh)

The tanh function maps input values to the range $(-1, 1)$ and is defined as:

$$\textbf{tanh}(z) = \frac{e^{z} - e^{-z}}{e^{z} + e^{-z}} \tag{2.7}$$

Compared to sigmoid, it is centered around zero, which can make learning more efficient in some contexts.

c) Rectified Linear Unit (ReLU) and Leaky ReLU

The Rectified Linear Unit (ReLU) is currently the most widely used activation function in deep learning due to its simplicity and computational efficiency. It is defined as:

$$\textbf{ReLU}(z) = \textbf{max}(0, z) \tag{2.8}$$

ReLU introduces non-linearity by passing positive inputs unchanged while setting negative inputs to zero.

However, it can lead to the *dying ReLU* problem, where some neurons output zero for all inputs and cease to learn. To address this, the Leaky ReLU variant was proposed. It modifies the original function to allow a small, non-zero gradient when the input is negative:

$$\textbf{Leaky ReLU}(z) = \begin{cases} z & \textbf{if } z > 0 \\ \alpha z & \textbf{if } z \leq 0 \end{cases} \tag{2.9}$$

where α is a small positive constant. This ensures that neurons remain active during training, even when receiving negative input values.

d) Softmax Function

The softmax activation function is commonly used in the output of classification networks when the goal is to predict the probability distribution over multiple classes.

$$\textbf{Softmax}(z_i) = \frac{e^{z_i}}{\sum_{j=1}^{K} e^{z_j}} \quad \text{for } i = 1, ..., K \tag{2.10}$$

Each output $\text{Softmax}(z_i)$ represents the predicted probability that the input belongs to class i. The softmax function ensures that all predicted probabilities are non-negative and sum to 1, forming a valid

probability distribution over the K possible classes. The class with the highest probability is then selected as the model's prediction, reflecting the category it considers most likely for the input.

The choice of activation functions can influence the performance of the network, and different layers or models may use different functions depending on the task at hand (Nwankpa et al., 2018).

2.2.3 Layered Structure of Deep Neural Networks

While individual artificial neurons form the basic computational units of deep learning models, it is their organization into *layers* that gives neural networks their expressive power. A typical deep neural network (DNN) is composed of an input layer, one or more hidden layers, and an output layer, forming a hierarchical structure in which each layer transforms the representation received from the previous one.

Figure 2.6: Schematic Representation of a Deep Neural Network

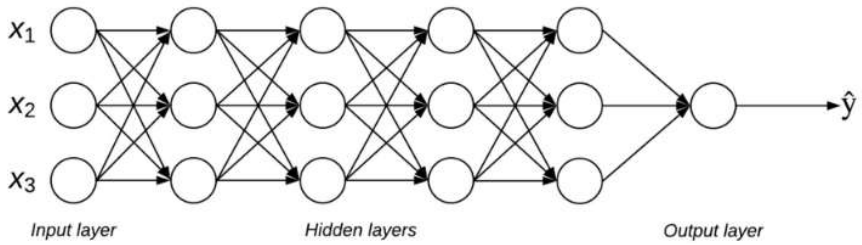

Source: (Jain et al., 2020)

The *input layer* introduces the raw features to the network, while the *hidden layers* apply non-linear transformations to learn internal representations, and the final *output layer* produces a prediction, whether a class label, probability distribution, or continuous value, depending on the task.

This layered organization enables the hierarchical feature learning that is characteristic of deep learning models: early layers capture low-level patterns, while deeper layers encode progressively higher-level abstractions. Such architectures have proven effective in a wide variety of domains, from image and speech recognition to time series modeling (LeCun et al., 2015).

2.2.4 Training Deep Neural Networks

a) Overview of the Learning Process

At the core of every deep neural network lies a large set of *weights* and associated *biases*, numerical parameters that determine how input data is transformed as it passes through the layers. These parameters define the behavior of each layer, and learning consists of finding values that enable the network to map inputs to desired outputs.

Training begins with weights set to random values, meaning the network initially performs poorly. To improve, it must receive feedback on how far off its predictions are from the correct answers. This feedback comes from the *loss function*, also sometimes called the *objective* or *cost function*, which measures the difference between the predicted output and the target. A high loss indicates poor performance, and a low loss suggests the network is making accurate predictions.

This loss value is then used by the *optimizer*, an algorithm that updates the weights to reduce it. It does so by computing how each weight contributes to the loss and adjusting them accordingly; this procedure is known as *backpropagation*. With each iteration, the network's weights are refined in small steps, gradually improving the network's predictions on both the training examples and unseen data.

Figure 2.7: Neural Networks Learning Process

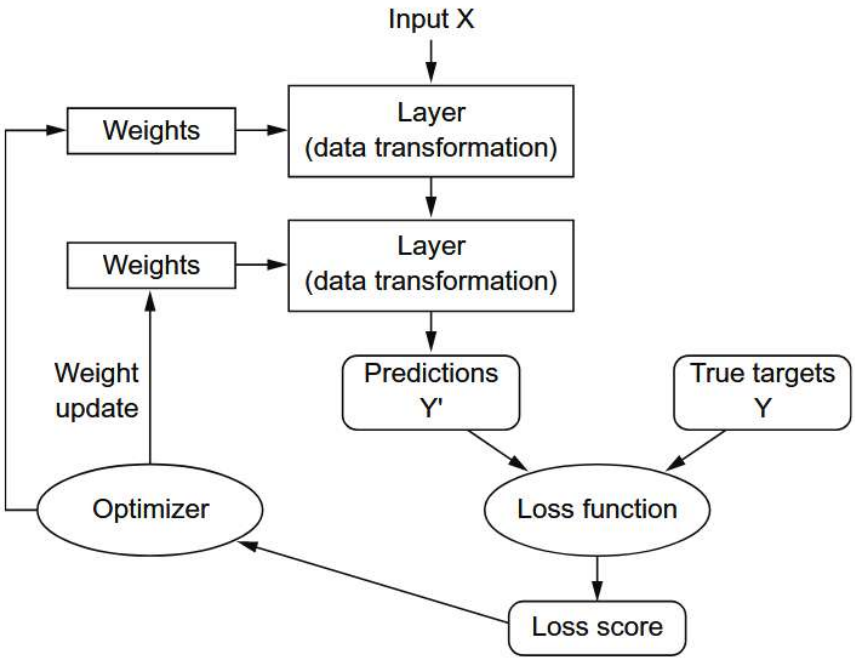

Source: (Chollet et al., 2022)

Through repeated exposure to data and many cycles of this process (Figure 2.7), the network converges to a configuration of weights that minimizes the loss, resulting in a model capable of making accurate predictions (Chollet et al., 2022).

b) Loss Functions

To guide a neural network toward producing accurate outputs, we must first establish a way to quantify how far its predictions deviate from the desired results. This is the role of the loss function, a mathematical expression that quantifies the difference between the network's predicted output and the actual target value for each training example. The loss function provides the guiding signal for learning: it determines how the model's parameters should be adjusted to improve performance (Chollet et al., 2022).

Different tasks require different types of loss functions:

- **Regression**

  In regression problems, where the network predicts continuous values, a common choice is the *Mean Squared Error* (MSE), It computes the average of the squared differences between predicted values and actual targets:

$$MSE = \frac{1}{n}\sum_{i=1}^{n}(\hat{y}_i - y_i)^2 \tag{2.11}$$

where $\hat{y}_i$ is the predicted value and y_i is the true value for the i^{th} training sample.

The squaring of errors ensures that larger deviations are penalized more heavily than smaller ones, making MSE sensitive to outliers. This characteristic is particularly valuable in regression tasks where minimizing large errors is crucial to performance.

Another commonly used metric is the *Root Mean Squared Error* (RMSE), defined as the square root of the MSE:

$$RMSE = \sqrt{\frac{1}{n}\sum_{i=1}^{n}(\hat{y}_i - y_i)^2} \tag{2.12}$$

While MSE and RMSE reflect the same underlying quantity, RMSE offers a more intuitive sense of how far off the predictions are, on average, by bringing the error back to the original unit of the target variable.

- **Classification**

  In classification problems, the preferred loss function is usually *cross-entropy loss*, which measures how well the predicted probability aligns with the true class labels. For binary classification, it takes the form:

$$\textbf{Binary Cross-Entropy} = -\frac{1}{n}\sum_{i=1}^{n}[y_i \log(\hat{y}_i) + (1 - y_i)\log(1 - \hat{y}_i)] \tag{2.13}$$

  where $\hat{y}_i \in [0, 1]$ is the predicted probability that sample i belongs to the positive class (1), typically produced by a sigmoid activation, and y_i is the true class label, 0 or 1.

  For multi-class classification tasks, where each input belongs to one among C possible classes, the binary formulation is extended to the *Categorical Cross-Entropy* loss:

$$\textbf{Categorical Cross-Entropy} = -\frac{1}{N}\sum_{i=1}^{N}\sum_{c=1}^{C} y_{i,c}\log(\hat{y}_{i,c}) \tag{2.14}$$

  $\hat{y}_{i,c}$ is the predicted probability that sample i belongs to class c, typically produced by a softmax activation function, and $y_{i,c}$ is the corresponding entry in the one-hot encoded true label vector for sample i. For instance, in a 3-class problem where the true label is class 2, the one-hot encoded vector would be $[0,\ 1,\ 0]$.

Loss functions are computed per training instance, and the total loss is typically calculated by averaging across all instances in a batch. The result is a single scalar value that summarizes the model's performance on that batch and serves as the feedback signal for updating the weights during training (Terven, Cordova-Esparza, Ramirez-Pedraza, Chavez-Urbiola, & Romero-Gonzalez, 2024).

In this way, the loss function defines the objective that the network seeks to minimize, transforming the abstract goal of making better predictions into a concrete mathematical problem that can be solved through optimization.

c) Gradient-Based Optimization

Training a neural network involves finding the set of parameters that minimize a loss function. This is done using gradient-based optimization, where the direction of steepest descent in the loss landscape is computed via derivatives. The foundational algorithm for this process is Gradient Descent (GD), which updates the model parameters θ iteratively based on the gradient of the loss $\mathcal{L}$ with respect to those parameters:

$$\theta \leftarrow \theta - \eta \nabla_\theta \mathcal{L} \tag{2.15}$$

where η is the learning rate that controls the step size.

Figure 2.8: Illustration of a Gradient Descent Path

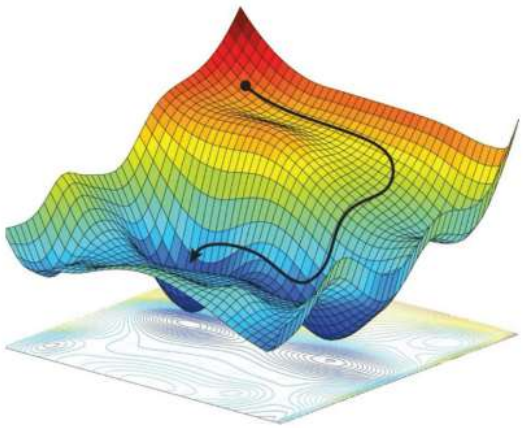

Source: (Argüelles & Collazo, 2023)

Depending on how much data is used to compute the gradient at each step, there are two common variants:

- **Batch Gradient Descent**: Computes the gradient using the entire training set. This ensures a stable update direction but becomes computationally expensive for large datasets.
- **Stochastic Gradient Descent (SGD)**: Rather than computing gradients over the entire dataset, SGD updates the model's parameters using only a subset of the data, typically a single sample or a mini-batch. This leads to faster, more frequent updates, which makes training more efficient, especially on large datasets. While the updates can be noisy due to the limited data used in each step, this noise often helps the model explore the solution space more effectively.

In standard gradient descent, the learning rate is fixed throughout training (Zhang, 2019). However, choosing the right learning rate is tricky: too small and training is slow; too large and the model may fail to converge. To address this, **adaptive optimizers** were introduced. These methods automatically

adjust the learning rate during training, depending on how the loss is behaving. This makes them more robust and effective, especially when dealing with noisy data or complex models.

Some widely used adaptive optimizers include:

- **AdaGrad** Adjusts how much the model learns from each step, allowing it to take smaller steps in directions it has already explored heavily, and larger steps where it still needs to learn more.
- **RMSProp** Improves on AdaGrad by keeping learning flexible over time, so the model can keep adjusting its steps without slowing down too much in directions it still needs to explore.
- **Adam** A popular optimizer that combines the strengths of AdaGrad and RMSProp, offering fast and reliable learning in most deep learning tasks.

These optimizers adapt their behavior over time and across parameters, which reduces the need for extensive manual tuning and often leads to faster convergence.

Limitations of Gradient-Based Methods

Among the issues gradient-based optimizers face:

- **Flat Regions and Critical Points**: These are areas in the loss surface where the gradient becomes very small or zero, such as saddle points. As a result, the optimizer may struggle to make progress and may fail to converge even to a local minimum.
- **Sensitivity to learning rate**: Even adaptive methods can struggle if the learning rate is poorly set, especially early in training.

Although reaching a global minimum is rarely guaranteed in deep learning, modern optimization techniques have significantly improved training stability and efficiency, enabling models to achieve strong performance in practice (Zhang, 2019).

d) Backpropagation: Efficient Gradient Computation

To optimize a neural network, the loss function's gradients must be calculated for every parameter. These gradients guide updates via gradient-based methods, progressively reducing the loss. This computation is performed efficiently using *backpropagation*. It can be described in two phases: a forward pass that computes the network's output, followed by a backward pass that propagates errors and calculates gradients.

Forward Pass.

Given an input vector $\mathbf{x} \in \mathbb{R}^n$, the neural network propagates the signal through each layer $l = 1, 2, \ldots, L$ using the following operations:

$$\mathbf{z}^{(l)} = \mathbf{W}^{(l)}\mathbf{a}^{(l-1)} + \mathbf{b}^{(l)} \tag{2.16}$$

$$\mathbf{a}^{(l)} = \boldsymbol{\phi}^{(l)}(\mathbf{z}^{(l)}) \tag{2.17}$$

where:

- $\mathbf{W}^{(l)}$ and $\mathbf{b}^{(l)}$ are the weight matrix and bias vector for layer l,
- $\mathbf{a}^{(l-1)}$ is the input to layer l (with $\mathbf{a}^{(0)} = \mathbf{x}$),
- $\phi^{(l)}(\cdot)$ is the activation function.

The final output $\hat{\mathbf{y}} = \mathbf{a}^{(L)}$ is compared with the ground truth $\mathbf{y}$ using a loss function $\mathcal{L}(\hat{\mathbf{y}}, \mathbf{y})$, producing a loss score.

Backward Pass: Applying the Chain Rule.

To update the parameters, we compute the gradient of the loss with respect to each weight and bias by recursively applying the chain rule. Let $\delta^{(l)} = \frac{\partial \mathcal{L}}{\partial \mathbf{z}^{(l)}}$ denote the error term at layer l.

- For the output layer $\boldsymbol{l = L}$:

$$\boldsymbol{\delta^{(L)} = \frac{\partial \mathcal{L}}{\partial \mathbf{a}^{(L)}} \odot \phi'^{(L)}(\mathbf{z}^{(L)})} \tag{2.18}$$

- For the hidden layers $\boldsymbol{l = L-1, L-2, \ldots, 1}$:

$$\boldsymbol{\delta^{(l)} = (\mathbf{W}^{(l+1)^\top} \delta^{(l+1)}) \odot \phi'^{(l)}(\mathbf{z}^{(l)})} \tag{2.19}$$

Here, $\odot$ denotes element-wise multiplication (Hadamard product), and $\phi'^{(l)}(\cdot)$ is the derivative of the activation function of layer l.

Gradient Computation.

Once the error signals $\delta^{(l)}$ are computed, the gradients with respect to the weights and biases are:

$$\frac{\partial \mathcal{L}}{\partial \mathbf{W}^{(l)}} = \delta^{(l)} \cdot \mathbf{a}^{(l-1)^\top} \tag{2.20}$$

$$\frac{\partial \mathcal{L}}{\partial \mathbf{b}^{(l)}} = \delta^{(l)} \tag{2.21}$$

These gradients are used to update the parameters:

$$\mathbf{W}^{(l)} \leftarrow \mathbf{W}^{(l)} - \eta \frac{\partial \mathcal{L}}{\partial \mathbf{W}^{(l)}} \tag{2.22}$$

$$\mathbf{b}^{(l)} \leftarrow \mathbf{b}^{(l)} - \eta \frac{\partial \mathcal{L}}{\partial \mathbf{b}^{(l)}} \tag{2.23}$$

where η is the learning rate.

Backpropagation is a computationally efficient method for gradient calculation in deep networks. By applying the chain rule layer by layer in reverse, the model can compute how each parameter contributes to the final error and how it should be updated to minimize this error. This mechanism is essential for training deep models using gradient-based optimization (Nielsen, 2015).

e) Hyperparameters

Training involves not only learning the model's weights and biases but also configuring a range of hyperparameters, settings that govern the learning process itself. Unlike learned parameters, hyperparameters are specified before training begins and are not updated during optimization. They play a critical role in shaping the model's performance, learning efficiency, and generalization ability (Kumar, Dalal, & Sethi, 2024).

Key hyperparameters in deep learning include:

- **Network Architecture**: The number of layers, the number of units per layer, and the choice of activation functions define the capacity of the model. Deeper and wider networks can represent more complex functions but also increase the risk of overfitting and computational cost.
- **Batch Size**: The number of training samples used to compute each gradient update. Smaller batch sizes often introduce more noise into the learning process, which can help escape local minima but may slow convergence. Larger batch sizes provide more stable gradient estimates but may require more memory and potentially lead to overfitting
- **Number of Epochs**: The number of times the entire training dataset is passed through the network. More epochs allow the model to learn more thoroughly, but excessive training may result in overfitting, especially in the absence of proper regularization.
- **Optimizer Choice and Configuration**: Different optimizers come with their own hyperparameters, such as momentum terms or decay rates, which can significantly affect training dynamics.
- **Learning Rate (η)**: This controls the size of the updates made to the model parameters at each step. A learning rate that is too small can lead to slow convergence, while a value that is too large may cause training to diverge or oscillate around a suboptimal solution.
- **Regularization Parameters**: These include dropout rate, L_1/L_2 weight penalties, and early stopping criteria. They help control overfitting by constraining the model's complexity or stopping training before it memorizes the training data.

Selecting appropriate hyperparameters is often a nontrivial task and typically requires empirical experimentation. Common strategies include:

- **Grid Search**: Exhaustively exploring combinations of hyperparameters over a specified range.
- **Random Search**: Sampling hyperparameter combinations randomly, which has been shown to be more efficient in high-dimensional spaces.
- **Bayesian Optimization**: Using probabilistic models to guide the search toward promising configurations.

Ultimately, careful tuning of hyperparameters is essential to unlock the full potential of a neural network. Poor choices can lead to underperforming models regardless of architecture, while well-chosen values can significantly improve learning speed, robustness, and generalization (Kumar et al., 2024).

2.3 Recurrent Neural Networks

Recurrent Neural Networks (RNNs) are a class of neural architectures specifically designed to model sequential data, where observations are temporally or contextually dependent. This makes RNNs particularly suited to time series forecasting, natural language processing, and any domain in which the order of data points carries meaningful information. In the context of wildfire forecasting, the time-evolving behavior of environmental variables such as temperature and humidity lends itself naturally to sequence modeling, where past observations influence current predictions.

2.3.1 RNN Architecture

Unlike feedforward neural networks, which assume that inputs are independent of one another, RNNs incorporate the concept of memory. They achieve this by maintaining a hidden state vector that is updated at each time step as new input is received. This recurrent connection allows information to persist across the sequence, enabling the model to capture temporal dynamics.

A basic RNN processes an input sequence $\{x_1, x_2, \ldots, x_T\}$ one element at a time, updating its internal hidden state h_t at each time step. The update is governed by a nonlinear activation function (tanh or ReLU) of the current input and the previous hidden state, as illustrated in figure 2.9.

Figure 2.9: A simple RNN, unrolled over time

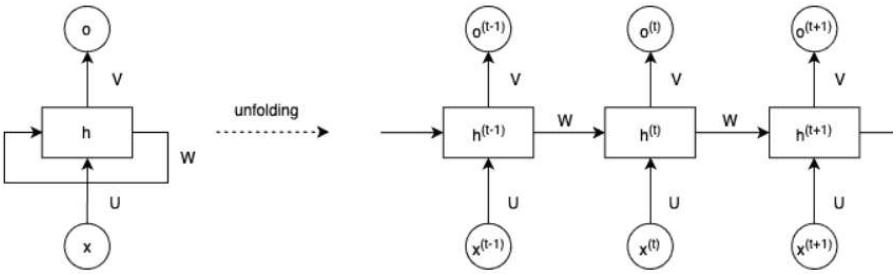

Source: Baeldung Retreived on May 29th

The hidden state is computed as:

$$h_t = \phi_h(Ux_t + Wh_{t-1} + b_h) \tag{2.24}$$

The output at each time step is computed as:

$$y_t = \phi_y(Vh_t + b_y) \tag{2.25}$$

where:

- $x_t \in \mathbb{R}^n$: input vector at time t.
- $h_t \in \mathbb{R}^m$: hidden state at time t.
- $y_t \in \mathbb{R}^k$: output at time t.
- U, W, V: weight matrices.
- b_h, b_y: bias vectors.

- ϕ_h, ϕ_y: activation functions.

This recurrence relation allows the network to carry information from the past (via h_{t-1}) into future computations. All weights are shared across time steps, which makes training efficient and ensures temporal consistency (Mienye, Swart, & Obaido, 2024).

2.3.2 Types of RNN Architectures

Recurrent Neural Networks (RNNs) can be configured in various architectural patterns depending on the nature of the input and output sequences. The most common RNN types include:

- **One-to-One**: The most basic type of neural network that produces a single output for a single input (e.g., image classification).
- **One-to-Many**: Takes a fixed-size input and produces a sequence of outputs (e.g., image captioning—takes an image as input and generates a descriptive sentence).
- **Many-to-One**: Takes a sequence of inputs and produces a fixed-size output (e.g., sentiment analysis).
- **Many-to-Many**: Takes a sequence of inputs and generates a sequence of outputs (e.g., machine translation).
- **Many-to-Many (Synchronized)**: Input and output sequences are synchronized (e.g., video classification to label each frame in a video).

Figure 2.10 illustrates these configurations visually.

Figure 2.10: Common RNN architecture configurations

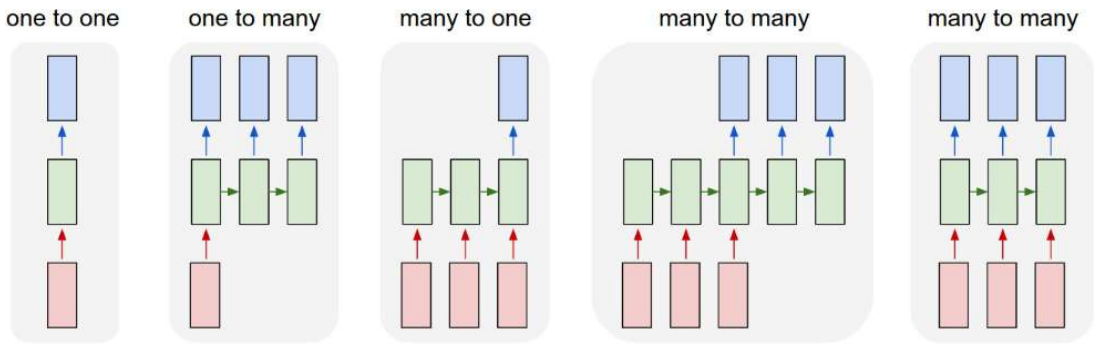

Source: Karpathy (2015) Retreived on May 29th

2.3.3 The Vanishing and Exploding Gradients Problem

Despite their conceptual simplicity, standard RNNs face challenges in capturing long-range dependencies due to the vanishing and exploding gradient problems, which hinder effective training on long sequences

When training an RNN, the model learns by adjusting its weights using a method called *backpropagation through time* (BPTT). This involves propagating error signals backwards through each time step in the sequence. In doing so, the gradients are multiplied repeatedly across time steps.

- If these gradients become very small, they can vanish. This means the model stops learning from earlier parts of the sequence because the error signals are too weak to have any effect. This is particularly problematic in tasks that require understanding of long-term dependencies, such as remembering weather conditions many days before a wildfire ignition.
- Conversely, if the gradients become very large, they can explode. This causes the model's weights to grow uncontrollably, leading to numerical instability and erratic learning. Exploding gradients can result in the model failing to converge or producing meaningless predictions.

These problems make it extremely difficult for standard RNNs to learn patterns that span long time intervals (Mienye et al., 2024).

2.3.4 Long Short-Term Memory Networks (LSTMs)

Long Short-Term Memory (LSTM) networks are a specialized type of Recurrent Neural Network introduced by Hochreiter and Schmidhuber (1997) to address the vanishing and exploding gradient problems that hinder the training of traditional RNNs on long sequences. LSTMs achieve this through a unique internal gating mechanism that allows them to learn which information to retain, update, or discard over time.

Figure 2.11: Architecture of LSTMs

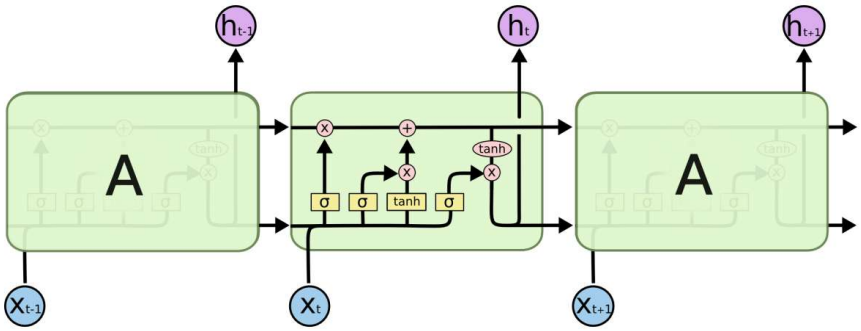

Source: (Olah, 2015)

Whereas basic RNNs use a single hidden state to carry temporal information, LSTMs augment this with an additional memory component: the *cell state*. This memory stream, minimally altered across time steps, enables LSTMs to propagate information over long distances. Three types of gates (forget, input, and output) regulate how much of the past should be retained, how much new information should be integrated, and what should be revealed to the rest of the network.

The LSTM Unit Functioning

At each time step t, the LSTM unit receives:

- The current input $\mathbf{x}_t \in \mathbb{R}^n$
- The previous hidden state $\mathbf{h}_{t-1} \in \mathbb{R}^m$
- The previous cell state $\mathbf{c}_{t-1} \in \mathbb{R}^m$

It then performs the following computations:

Figure 2.12: The LSTM Unit

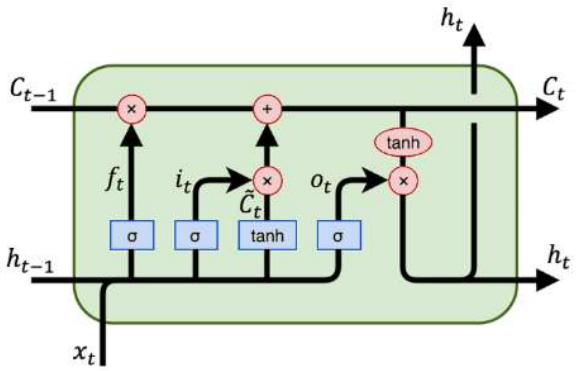

Source: (Olah, 2015)

Forget Gate ($\mathbf{f}_t$)

$$\mathbf{f}_t = \sigma(\mathbf{W}_f \mathbf{x}_t + \mathbf{U}_f \mathbf{h}_{t-1} + \mathbf{b}_f) \tag{2.26}$$

This gate decides which parts of the previous cell state $\mathbf{c}_{t-1}$ should be forgotten. Values close to 0 result in forgetting, while values near 1 retain information.

Input Gate ($\mathbf{i}_t$) and Candidate Memory ($\tilde{\mathbf{c}}_t$)

$$\mathbf{i}_t = \sigma(\mathbf{W}_i \mathbf{x}_t + \mathbf{U}_i \mathbf{h}_{t-1} + \mathbf{b}_i) \tag{2.27}$$

$$\tilde{\mathbf{c}}_t = \tanh(\mathbf{W}_c \mathbf{x}_t + \mathbf{U}_c \mathbf{h}_{t-1} + \mathbf{b}_c) \tag{2.28}$$

The input gate determines which new information to write to memory, and $\tilde{\mathbf{c}}_t$ is the candidate content.

Update the Cell State ($\mathbf{c}_t$)

$$\mathbf{c}_t = \mathbf{f}_t \odot \mathbf{c}_{t-1} + \mathbf{i}_t \odot \tilde{\mathbf{c}}_t \tag{2.29}$$

This update equation blends the previous cell state with the new candidate values.

Output Gate ($\mathbf{o}_t$) and Hidden State Update ($\mathbf{h}_t$)

$$\mathbf{o}_t = \sigma(\mathbf{W}_o \mathbf{x}_t + \mathbf{U}_o \mathbf{h}_{t-1} + \mathbf{b}_o) \tag{2.30}$$

$$\mathbf{h}_t = \mathbf{o}_t \odot \tanh(\mathbf{c}_t) \tag{2.31}$$

The output gate controls which parts of the updated memory are exposed to the hidden state, which is used for downstream predictions or passed to the next time step.

Where, σ denotes the sigmoid activation function, tanh is the hyperbolic tangent function, and $\odot$ represents element-wise multiplication. All weight matrices and biases are learned during training and are shared across all time steps (Olah, 2015).

3 Explainable Artificial Intelligence (XAI)

As machine learning systems become increasingly integrated into high-stakes decision-making processes, the need for transparency and interpretability has become a must. While traditional models like decision trees or logistic regression offer inherent interpretability, modern deep learning models, such as LSTMs operate as *black boxes*, making it difficult to understand how predictions are derived (Lipton, 2018). This problem raises concerns in sensitive domains, such as wildfire forecasting, where understanding the reasoning behind a prediction can be just as critical as the prediction itself.

Explainable Artificial Intelligence **(XAI)** refers to a set of techniques and frameworks designed to make the behavior and decisions of machine learning models more understandable to humans. The goal is to ensure accountability by enabling the tracing and justification of model decisions, fairness by preventing systematic bias against specific groups or conditions, and robustness by ensuring reliable performance under varying or unforeseen inputs (Doshi-Velez & Kim, 2017).

3.1 Categories of Explainability

Explainability in machine learning can be classified based on two main criteria: when the explanation is introduced (intrinsic vs. post-hoc) and what aspect of the model it targets (global vs. local). These distinctions are crucial when selecting appropriate interpretability approaches (Abdullah, Zahid, & Ali, 2021).

3.1.1 Intrinsic vs. Post-hoc Interpretability

Intrinsic interpretability refers to models whose structure is inherently understandable to humans. Examples include decision trees and linear models, where the decision-making logic is transparent by design. These models sacrifice some predictive power for interpretability, making them suitable when transparency is a strict requirement.

In contrast, post-hoc interpretability involves applying external methods to explain black-box models such as deep neural networks or ensemble methods. Post-hoc techniques aim to extract insights from already trained models without altering their internal architecture, like feature importance scores.

3.1.2 Global vs. Local Explanations

Global explanations aim to describe the overall behavior of a model across the entire input space. These explanations help users understand general model trends and decision boundaries, for example, which features are most influential on average or how the model prioritizes variables across all samples.

Local explanations, on the other hand, focus on individual predictions. They provide insight into why a model made a specific decision for a particular input instance. Local methods are essential when users must examine decisions case-by-case, as in clinical diagnosis.

Both types of explanations are complementary. Global explanations promote understanding at the system level, while local explanations are critical for transparency in individual, high-impact decisions.

3.2 XAI Methods: Integrated Gradients and Permutation Feature Importance

A wide range of interpretability methods has been developed to address the opacity of complex machine learning models. These methods can broadly be classified as either *model-specific* or *model-agnostic*. Model-specific approaches are tailored to particular model architectures and exploit their internal structure, such as gradients, to generate explanations. In contrast, model-agnostic techniques operate independently of the underlying model and treat it as a black box, relying solely on input-output behavior (Abdullah et al., 2021). In this study, two complementary interpretability methods are employed: Integrated Gradients, a model-specific technique designed for neural networks, and Permutation Feature Importance, a model-agnostic approach applicable to any predictive model.

3.2.1 Integrated Gradients

Integrated Gradients (IG) is a gradient-based attribution method designed to explain the predictions of deep neural networks. Proposed by Sundararajan, Taly, and Yan (2017), it addresses some core limitations of standard gradient-based explanations, particularly the issue of saturation, where the gradient at the input may be close to zero even when a feature is highly influential.

The idea behind IG is to assess not just how sensitive the output is at the input point, but to average this sensitivity along a path from a baseline input (like an all zero vector) to the actual input. In other words, as each feature goes from zero to its actual value, the method observes how the model's output, such as fire probability, changes along the way. Mathematically, this is done by integrating the gradients of the model output with respect to the input features across these intermediate steps.

In doing so, IG provides a more reliable and theoretically grounded measure of feature importance that accounts for the cumulative effect of each input on the model's decision.

The following steps show the Integrated Gradients computation:

Step 1: Define the Input and Baseline

Let:

- $\mathbf{x} = [x_1, x_2, \ldots, x_n]$ be the actual input vector (e.g., one 30-day wildfire sample, flattened),
- $\mathbf{x}' = [x'_1, x'_2, \ldots, x'_n]$ be the baseline input vector (e.g., all zeros or mean feature values),
- $F(\mathbf{x})$ be the scalar output of the model for input $\mathbf{x}$ (e.g., probability of fire ignition).

Step 2: Interpolated Inputs

Construct $\mathbf{m}$ interpolated inputs between $\mathbf{x}'$ and $\mathbf{x}$:

$$\mathbf{x}^{(k)} = \mathbf{x}' + \frac{k}{m}(\mathbf{x} - \mathbf{x}'), \quad \text{for } k = 1, 2, \ldots, m \tag{2.32}$$

Each $\mathbf{x}^{(k)}$ represents a step along the path from the baseline to the actual input.

Step 3: Compute Gradients

For each interpolated input $\mathbf{x}^{(k)}$, compute the gradient of the model output with respect to input:

$$\nabla_x F(\mathbf{x}^{(k)}) = \left[\frac{\partial F}{\partial x_1}(\mathbf{x}^{(k)}), \ldots, \frac{\partial F}{\partial x_n}(\mathbf{x}^{(k)})\right] \tag{2.33}$$

Step 4: Average the Gradients

Approximate the integral by computing the average gradient for each feature over the m steps:

$$\mathbf{AvgGrad}_i = \frac{1}{m}\sum_{k=1}^{m}\frac{\partial F(\mathbf{x}^{(k)})}{\partial x_i} \tag{2.34}$$

Step 5: Integrated Gradients Attribution

Multiply the average gradient by the difference between the input and the baseline for each feature:

$$\mathbf{IG}_i(\mathbf{x}) = (x_i - x_i') \cdot \mathbf{AvgGrad}_i \tag{2.35}$$

Substituting the expression for AvgGrad_i yields the final IG formula:

$$\mathbf{IG}_i(\mathbf{x}) = (x_i - x_i') \cdot \frac{1}{m}\sum_{k=1}^{m}\frac{\partial F\left(\mathbf{x}' + \frac{k}{m}(\mathbf{x} - \mathbf{x}')\right)}{\partial x_i} \tag{2.36}$$

Which an approximation for the orginal IG formula:

$$\mathbf{IG}_i(\mathbf{x}) = (x_i - x_i') \cdot \int_{\alpha=0}^{1}\frac{\partial F(\mathbf{x}' + \alpha(\mathbf{x} - \mathbf{x}'))}{\partial x_i}\, d\alpha \tag{2.37}$$

Where $\alpha \in [0, 1]$ is a scaling factor that linearly interpolates between the baseline $\mathbf{x}'$ (when $\alpha = 0$) and the actual input $\mathbf{x}$ (when $\alpha = 1$).

3.2.2 Permutation Feature Importance

Permutation Feature Importance (PFI) is a model-agnostic method for estimating the importance of individual input features in a predictive model. First introduced by Breiman (2001) in the context of random forests, the approach has since become a general-purpose tool for post-hoc model interpretation (Molnar, 2025). The key idea is to measure how much the model's predictive performance deteriorates when the values of a specific feature are randomly permuted, thereby breaking any relationship between that feature and the target.

If permuting a feature results in a significant drop in performance (e.g., AUC, precision), then the model relied heavily on that feature to make accurate predictions. In contrast, if the performance remains largely unchanged, the feature is likely uninformative or redundant.

PFI is especially useful for understanding global feature importance, that is, how important each feature is on average across the entire test set, rather than for a specific sample. Below, we outline the steps of this method.

Step 1: Define Notation

Let:

- $\mathcal{D} = \{(\mathbf{x}^{(j)}, y^{(j)})\}_{j=1}^{N}$ be the dataset of N input-output pairs,
- $F(\cdot)$ be the trained model, and $\mathcal{M}(\mathcal{D}, F)$ a metric evaluating model performance (e.g., AUPRC),
- $\mathbf{x}_i$ refer to the i-th feature column across all N samples.

Step 2: Compute Baseline Performance

First, compute the model's original performance on the unaltered dataset:

$$\textbf{Baseline} = \mathcal{M}(\mathcal{D}, F) \tag{2.38}$$

Step 3: Permute Feature Values

For each feature x_i, create a perturbed version of the dataset $\mathcal{D}_{\text{perm}(i)}$ by randomly permuting the values in feature x_i, keeping all other features unchanged.

Step 4: Evaluate Model Performance on Permuted Data

Evaluate the model performance on the permuted dataset:

$$\textbf{Perf}_{\text{perm}(i)} = \mathcal{M}(\mathcal{D}_{\text{perm}(i)}, F) \tag{2.39}$$

Step 5: Compute Importance Score

The permutation importance score for feature x_i is computed as the performance drop:

$$\textbf{PFI}_i = \textbf{Baseline} - \textbf{Perf}_{\text{perm}(i)} \tag{2.40}$$

A larger $\textbf{PFI}_i$ indicates a greater contribution of feature x_i to the model's predictive performance.

This procedure is typically repeated multiple times with different random permutations to reduce noise, and the final importance score is averaged over runs (Molnar, 2025).

Conclusion

This chapter has established the conceptual and methodological groundwork for the wildfire prediction model developed later in this work. It began by presenting the core principles of machine learning, including supervised and unsupervised methods, introduced key challenges in model training and evaluation, including overfitting, data leakage, and class imbalance and highlighted the relevance of deep learning architectures, particularly recurrent networks such as LSTMs, for modeling spatiotemporal patterns. Finally, the chapter explored the critical role of explainability in predictive modeling, emphasizing the necessity of interpretability techniques to ensure model transparency and support decision-making in high-risk applications. Together, these foundations provide the essential context for understanding the modeling pipeline and evaluation strategies that follow in Chapter 3.

CHAPTER 3:

Wildfire Risk Predicition in the Mediterranean Basin

Chapter 3

Wildfire Risk Predicition in the Mediterranean Basin

Introduction

This chapter presents the modeling framework developed to predict large wildfire ignitions using the Mesogeos dataset. Building on the insights from the Exploratory Data Analysis (EDA), which highlighted key spatial, seasonal, and variable-specific fire patterns, we developed a deep learning pipeline to capture the spatiotemporal structure of wildfire drivers.

After handling missing values and engineering relevant features, the data was split, and a Long Short-Term Memory (LSTM) model was then trained to estimate ignition probabilities.

Model performance was evaluated using multiple metrics, with emphasis on AUPRC and recall. Finally, we applied Integrated Gradients and Permutation Feature Importance to interpret the model's behavior and identify the most influential predictors over time.

1 Dataset Characterization and Exploration

1.1 Data Description

The data used in this study comes from the **Mesogeos Dataset**, developed by Kondylatos, Prapas, Camps-Valls, and Papoutsis (2023), presented at the NeurIPS 2023 Datasets and Benchmarks Track. The dataset brings together a diverse set of 27 features known to influence wildfire risk, grouped into four main categories:

- **Meteorological variables:** These include air temperature at 2 meters above the ground (t2m), land surface temperature at day and night (lst_day, lst_night), dew point temperature (d2m), relative humidity (rh), wind speed and direction, total precipitation (tp), surface pressure (sp), and surface solar radiation downwards (ssrd), capturing daily atmospheric conditions that affect ignition probability and fire spread.
- **Topographic variables:** Elevation (dem), slope, aspect, and terrain curvature, describing the physical landscape, which influences how fire behaves once ignited.

- **Vegetation and land cover indicators:** The dataset includes the leaf area index (lai), normalized difference vegetation index (ndvi), soil moisture index (smi), and a set of fractional land cover proportions (lc_*), representing the share of each $1km^2$ grid cell occupied by different land cover types such as forests, grasslands, and agricultural areas.
- **Human-related features:** These include population density and distance to the nearest road, representing anthropogenic factors.

Table 3.1: Features Description

Variable	Description	Unit
`t2m`	Air temperature at 2 meters	K
`lst_day`	Land surface temperature (daytime)	K
`lst_night`	Land surface temperature (nighttime)	K
`d2m`	Dew point temperature (proxy for air humidity)	K
`rh`	Relative humidity	[0–1]
`wind_speed`	Wind speed	m/s
`wind_direction`	Wind direction (clockwise from North)	degrees
`tp`	Total daily precipitation	m
`sp`	Surface atmospheric pressure	Pa
`ssrd`	Surface solar radiation downwards	J/m^2
`dem`	Elevation above sea level	m
`slope`	Terrain slope	radians
`aspect`	Terrain aspect (orientation of slope)	degrees
`curvature`	Terrain curvature (concavity or convexity)	radius
`lai`	Leaf Area Index (proxy for vegetation density)	m^2/m^2
`ndvi`	NDVI (proxy for vegetation greenness and health)	[–1 to 1]
`smi`	Soil Moisture Index	[0–1]
`population`	Population density	people/km^2
`roads_distance`	Distance to nearest road	km
`lc_*`	Fractional land cover proportions (e.g., forest, agriculture, water)	[0–1]

Source: Produced by the author using `LaTeX`

The dataset is structured into individual samples, each representing a 1 km^2 grid cell and spanning a 30-day time window of daily observations across all variables. These windows end on the day $(t-1)$ before the ignition day, and the associated binary target variable **fire_occurred** indicates whether a wildfire ignition took place on day (t). A value of 1 corresponds to a **positive** sample, indicating the occurrence of a large fire ignition (>30 hectares), while a value of 0 denotes a **negative** sample with no fire ignition. Topographic and human-related features are static, remaining constant across the entire window for each sample. This structure yields a total of 25,916 samples and 777,480 rows, with each row corresponding to one day of observation within a sample window.

1.2 Exploratory Data Analysis

Exploratory Data Analysis (EDA) is a fundamental practice in data investigation. It provides an approach to explore and summarize data to uncover hidden relationships and patterns. Through the use of visualizations and basic statistical methods, EDA enables an in-depth examination of the data, often revealing trends, associations, and anomalies that would otherwise go unnoticed.

1.2.1 Fire Occurrence Patterns

To understand the conditions that lead to large wildfires, we begin by examining the distribution and patterns of fire occurrences in the dataset. This foundational step highlights both the temporal and spatial dynamics of fire ignition, as well as the balance of event classes in the modeling task.

a) Distribution of Fire and Non-Fire Samples

Out of 25,916 samples, 8,574 correspond to fire events, while 17,342 are non-fire samples. This yields a fire occurrence proportion of approximately 33%, reflecting a moderate class imbalance in the dataset, where the number of non-fire samples is nearly twice that of fire samples.

Figure 3.1: Distribution of fire and non-fire samples in the dataset.

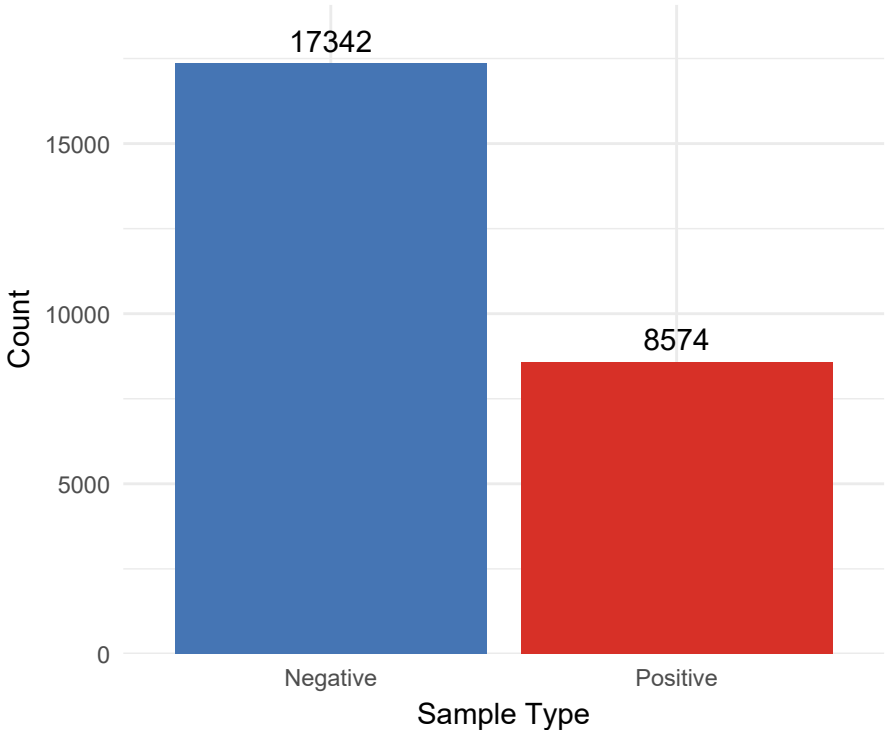

Source: Produced by the author using R.

This imbalance is expected given the nature of the problem: large wildfires are relatively rare events compared to the vast number of spatiotemporal points that do not experience ignition. Understanding this distribution is important as it emphasizes how rare, but significant, large fire events are, and underscores the importance of identifying them in contrast to the much more frequent non-fire days.

b) Seasonal Distribution of Fire Ignitions

An analysis of fire occurrence across months reveals a highly seasonal pattern. The number of fire samples rises sharply in summer, peaking in August (3,507) and July (2,504). Together, these two months account for approximately 70% of all fire samples in the dataset.

Figure 3.2: Monthly distribution of fire ignition samples.

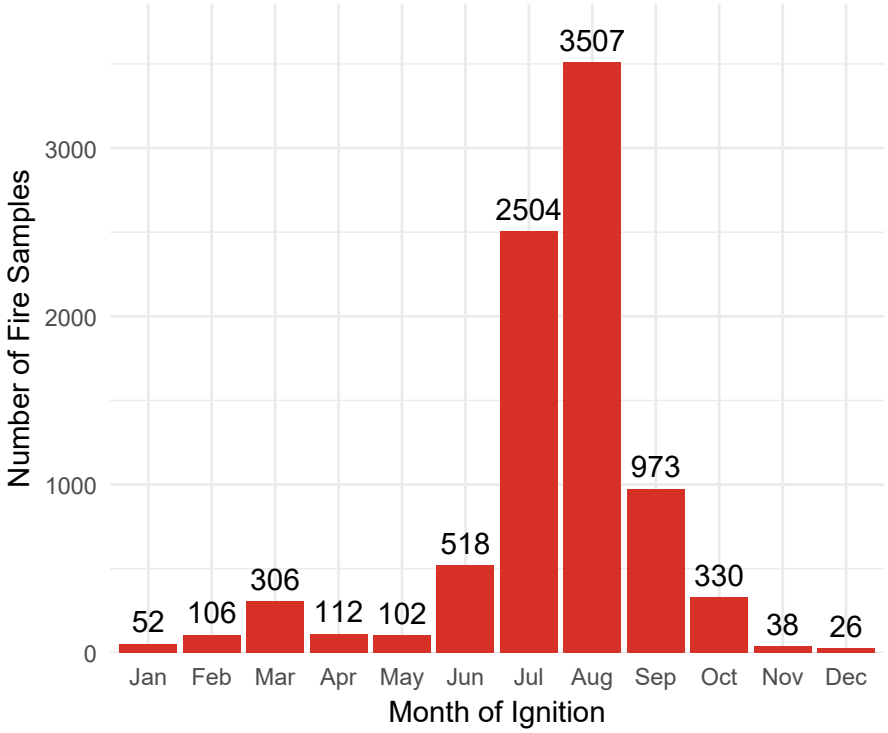

Source: Produced by the author using R

The chart confirms the seasonal nature of large wildfires in the Mediterranean region, with fire events concentrated almost entirely in the summer months (June–September). This pattern reflects the combined influence of heat, prolonged dryness, and fuel availability during this period, which amplifies wildfire risk.

c) Spatial Distribution of Fire Ignitions

The spatial distribution of fire samples indicates that ignitions are not randomly spread across the study area. Rather, they tend to cluster in specific regions, suggesting underlying spatial dependencies potentially linked to land cover types, topographic features, meteorological conditions, or human activities.

Figure 3.3: Spatial distribution of fire ignition samples.

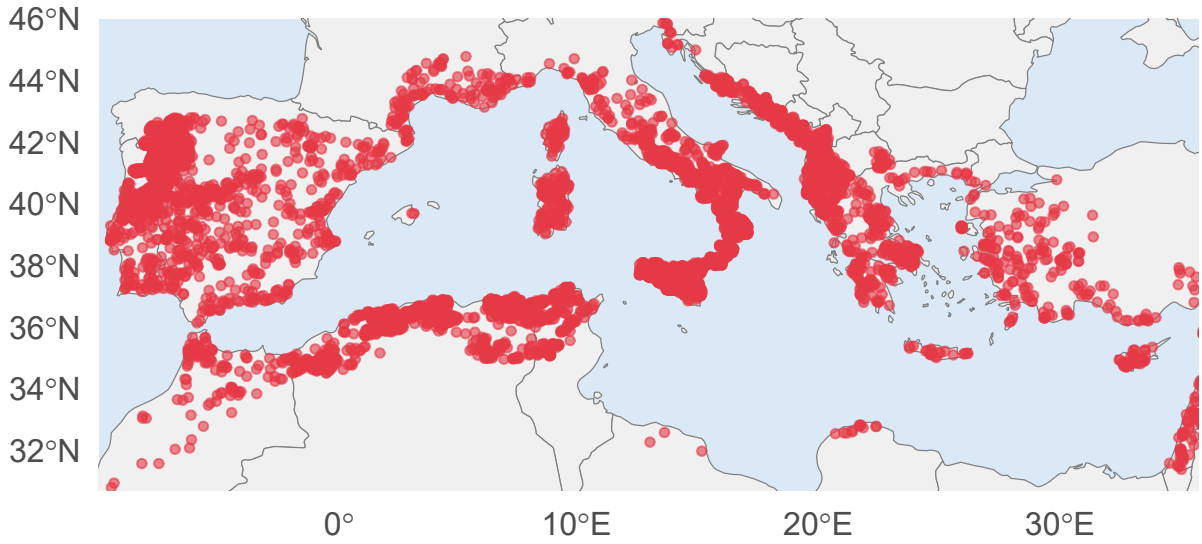

Source: Produced by the author using R

The map illustrates that most large fire ignitions are concentrated along the northern rim of the Mediterranean Basin, particularly in countries such as Spain, Portugal, Italy, and Greece. These areas exhibit a high density of ignition points, whereas large portions of North Africa and the Eastern Mediterranean show notably fewer events. This spatial contrast likely corresponds to differences in vegetation patterns, land use intensity, and fire management practices across the region.

1.2.2 Predictors Dynamics

Having understood where and when fires tend to occur, we next investigate whether distinct patterns emerge between negative and positive samples.

a) Dynamic Features

Starting with dynamic features, we first focus on the temporal behavior of key meteorological variables over the 30 days preceding the day of interest.

Before constructing the visualization, we filtered the dataset to retain only samples from the summer months (June to September), which correspond to the peak fire season in the Mediterranean. This restriction ensures that fire and non-fire samples are compared within a similar seasonal context, minimizing the influence of confounding factors introduced by seasonal variability in meteorological conditions. For instance, comparing summer fire events to non-fire samples from winter could lead to misleading conclusions, as differences in variables such as temperature or humidity might simply reflect normal seasonal shifts rather than factors associated with fire occurrence. The resulting subset consisted of 7,502 fire samples and 7,956 non-fire samples, a nearly balanced distribution, therefore eliminating the need for further sampling adjustments.

Figure 3.4: Mean Temporal Trajectories of Key Meteorological Variables During Fire Season

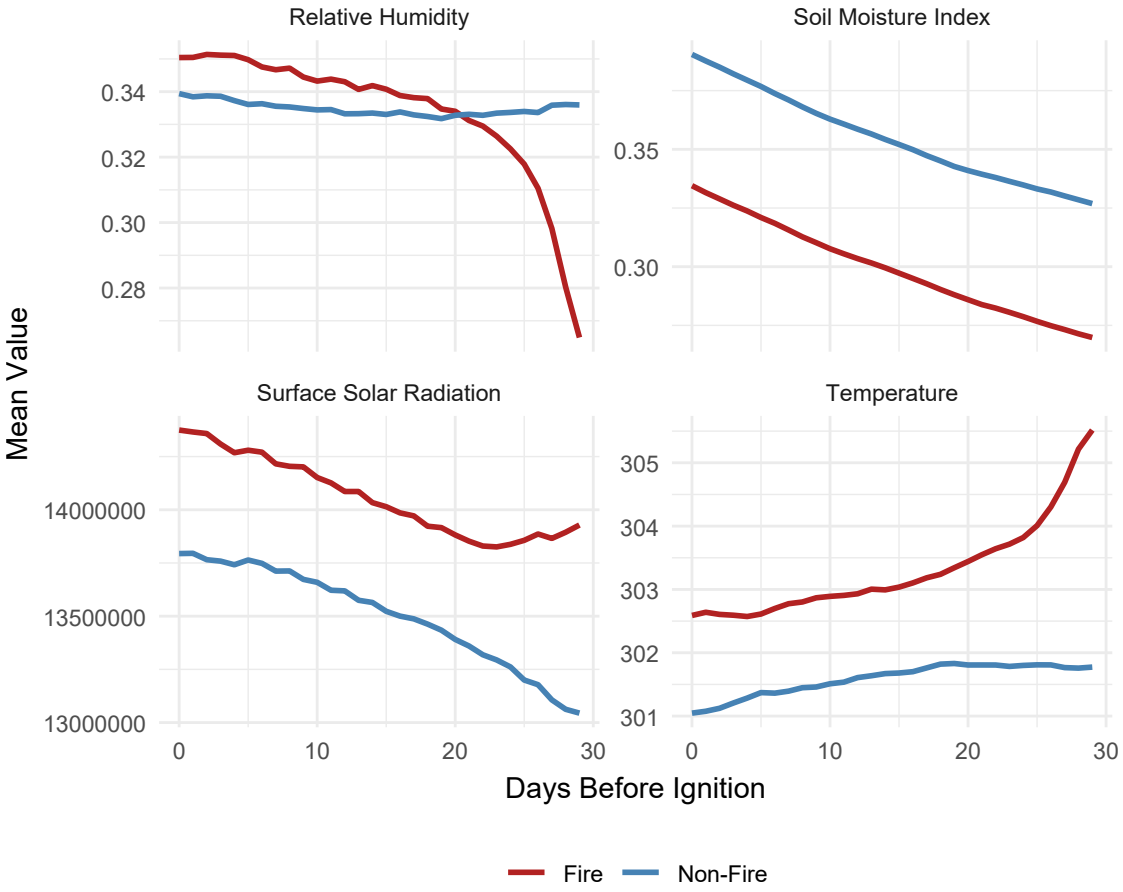

Source: Produced by the author using R

Figure 3.4 reveals clear differences between fire and non-fire samples. Fire samples are characterized by lower relative humidity (RH) and soil moisture index (SMI), and higher 2-meter air temperature (T2M) and surface solar radiation (SSRD), conditions known to favor combustion.

In the days leading up to ignition, RH and SMI in fire samples decline steadily, with RH dropping sharply in the final week. This reflects increasing atmospheric and soil dryness, a typical precursor to wildfire. Non-fire samples also show a gradual decrease in SMI, due to seasonal drying during the summer months, but the trend is less pronounced, and RH remains relatively stable.

T2M shows a noticeable upward trend in fire samples, especially in the last few days, whereas in non-fire samples it stays approximately flat. Similarly, SSRD rises more sharply in fire samples, suggesting enhanced surface heating, which accelerates fuel drying.

We also explored off-season samples and found that the trajectories exhibited similar patterns, with slightly lower temperatures and higher humidity, which is consistent with expectations outside the summer months. These dynamics are consistent with real-world observations of fire-weather interactions in the Mediterranean Basin, where large fire outbreaks often follow cumulative stress from heatwaves, low humidity, and prolonged rain-free periods.

In figure 3.5, using the full dataset, we present the meteorological and vegetation features distributions to further support the observed differences between positive and negative samples.

Figure 3.5: Distributions of Meteorological and Vegetation Variables

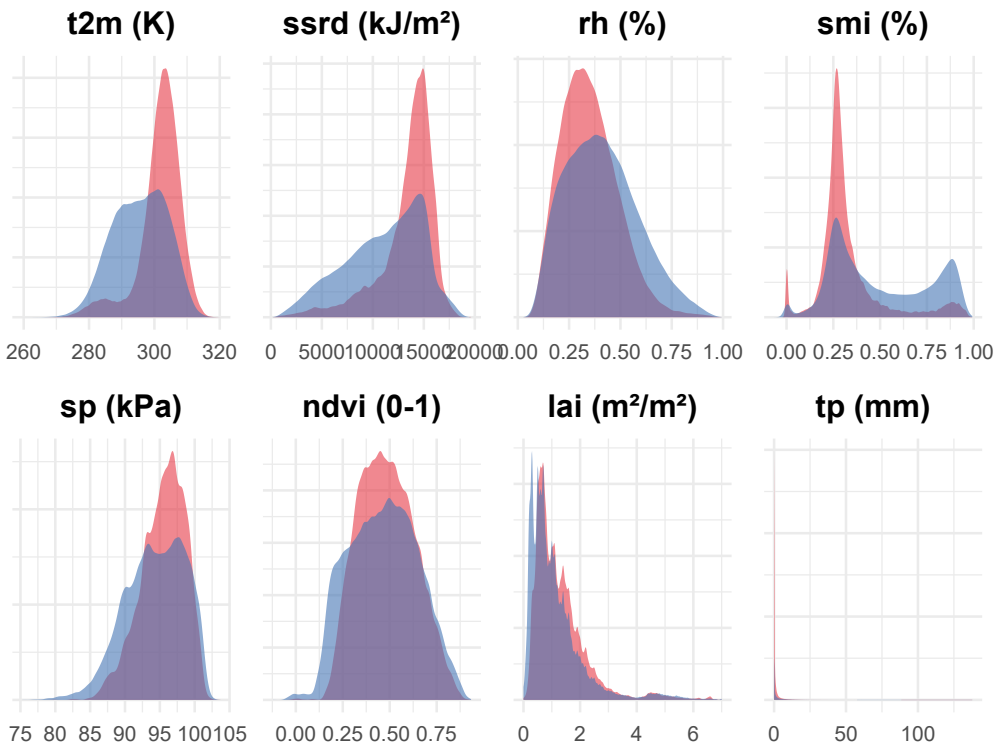

Source: Produced by the author using R

Temperature (t2m) and surface solar radiation (ssrd) distributions reveal a clear separation between fire and non-fire samples, with fire samples associated with higher temperatures and surface heating, which supports vegetation flammability and accelerates fuel drying.

Fire samples exhibit systematically lower values for both relative humidity (rh) and soil moisture content (smi), reflecting the drier atmospheric and soil conditions that promote fire ignition and spread. Notably, the separation is most pronounced for smi, suggesting that it may be one of the most reliable indicators of fire risk.

For atmospheric variables, fire samples are associated with higher surface pressure (sp), consistent with stable, high-pressure systems that suppress precipitation and favor prolonged dry spells. Conversely, total precipitation (tp) shows the expected inverse relationship, with fire samples skewed toward lower values, reinforcing the critical role of rainfall deficits in creating conditions conducive to fire activity.

Vegetation characteristics also exhibit notable trends. Fire samples correspond to moderate NDVI values, suggesting intermediate fuel loads that balance flammability and connectivity, while lower LAI values indicate sparser canopy cover, which can facilitate fuel drying and ignition.

Overall, the distributions reinforce the findings from the temporal analysis, highlighting the interplay of high temperatures, low humidity, and dry vegetation as key drivers of fire occurrence. The clear separation between fire and non-fire samples across multiple variables underscores the robustness of these predictors in distinguishing fire-prone conditions.

b) Static Features

In addition to dynamic atmospheric and vegetation conditions, certain fixed landscape features play a critical role in shaping baseline fire susceptibility, particularly topography, land cover, and human accessibility, which can help explain where fires are more likely to ignite under favorable conditions.

Figure 3.6: Elevation Distibution

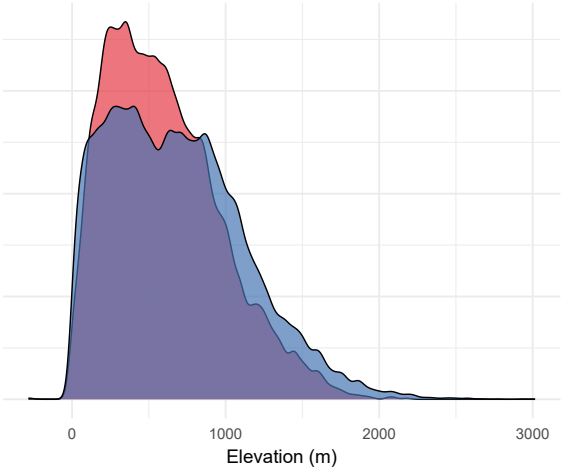

Figure 3.7: Mean Land Cover Proportions in Fire Samples

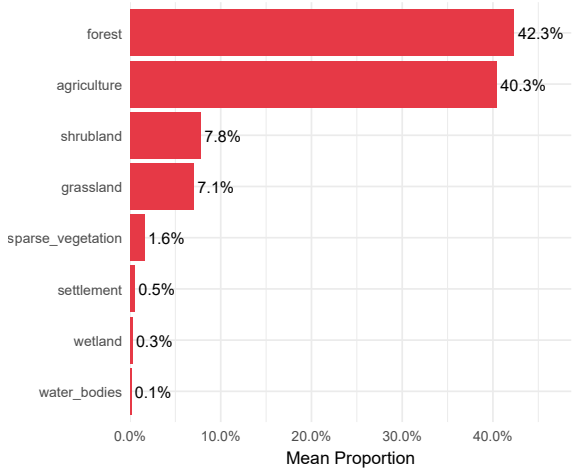

Source: Produced by the author using R

The land cover distribution among fire samples reveals a strong dominance of forests (42.3%) and agriculture (40.3%), together accounting for over 80% of the landscape where large fires occurred. Other vegetation types like shrubland (7.8%) and grassland (7.0%) follow, while settlements, wetlands, and water bodies represent only marginal proportions.

This suggests that fire-prone areas in the Mediterranean are largely composed of dense or semi-managed vegetated ecosystems, like forests and farmlands. The low presence of wetlands and water bodies is expected, given their fire-suppressive characteristics.

Elevation distribution plot complements figure 3.7, showing that fires predominantly occur at mid elevations, with a noticeable density peak between 200 and 800 meters, while non-fire samples are more widely dispersed. This elevation range often overlaps with forested and rural agricultural zones, where fuel is abundant and human presence, though less dense than in urban areas, remains non-negligible. In the dataset, the average road distance further reinforces this, with fire samples located closer to roads (3.09km) than non-fire samples (3.43km), suggesting that areas accessible by roads may have higher ignition risks due to human activity.

To contextualize these patterns geographically, Figure 3.8 presents a spatial map of elevation across the Mediterranean Basin. When considered alongside Figure 3.3, the overlap between mid-elevation zones and fire-prone regions becomes evident, reinforcing how topography shapes ignition potential.

Figure 3.8: Spatial Distribution of Elevation

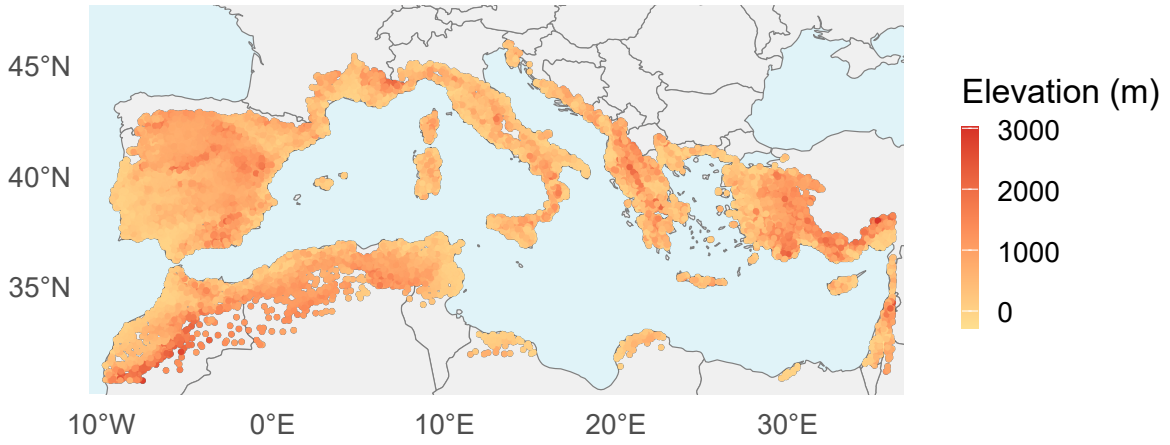

Source: Produced by the author using R

Overall, the plots together suggest that large wildfires tend to emerge in fuel-rich, vegetated areas at intermediate elevations, possibly where climatic conditions, vegetation type, and human activity intersect most critically.

Beyond elevation, the orientation of slopes also affects fire risk through differential solar exposure. South-facing slopes, which receive the most sunlight in the Northern Hemisphere, tend to dry out faster and support more flammable microclimates.

Figure 3.9: Fire Count by Slope Orientation

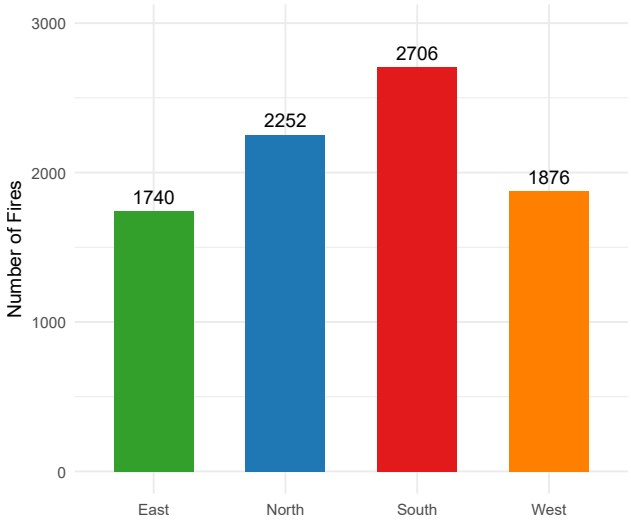

Source: Produced by the author using R

This is clearly reflected in Figure 3.9, which shows the highest number of fire ignitions on south-facing slopes, followed by north-facing ones. While north-facing slopes may retain more moisture, they also support denser vegetation, which can accumulate large fuel loads over time. East- and west-facing slopes display fewer ignitions, possibly due to more balanced exposure and lower extremes in fuel desiccation.

1.2.3 Correlation Analysis

To examine interdependencies among predictors and identify potential multicollinearity, we computed Pearson correlation coefficients between a selected set of continuous variables. They were aggregated across the 30-day window preceding each sample, using mean values to reduce daily variability. Directional variables such as wind direction and aspect were excluded from this analysis due to their circular nature, which violates linear correlation assumptions. Likewise, spatial coordinates and compositional land cover variables were excluded from this analysis.

Figure 3.10: Pearson Correlation Matrix of Key Predictors Related to Wildfire Risk

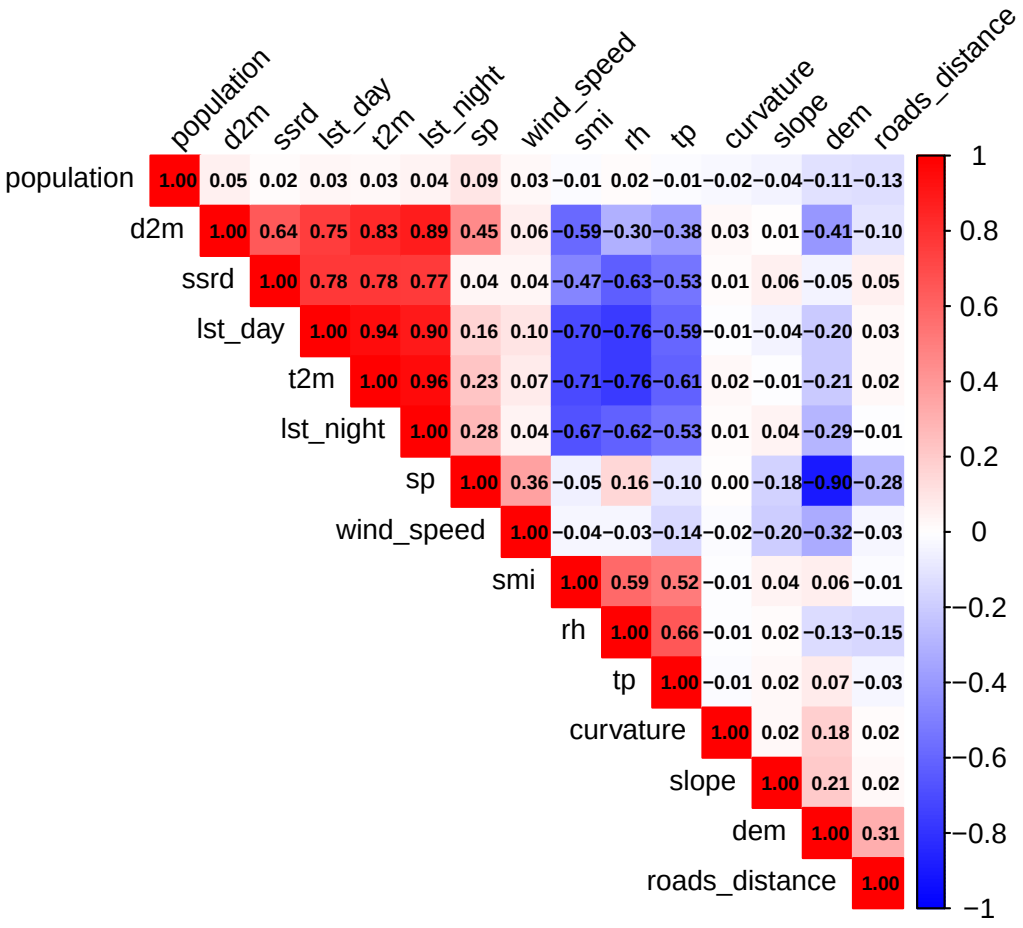

Source: Produced by the author using R

As expected, Temperature-related variables (t2m, lst_day, lst_night) are highly correlated ($r > 0.94$), indicating overlapping thermal information and suggesting that only one may be retained during modeling to avoid redundancy. Moisture indicators (rh, smi, tp) are positively associated and exhibit strong negative correlations with temperature and solar radiation, reinforcing the classic fire-conducive pattern of simultaneous heat and dryness. Vegetation indices (ndvi, lai) provide additional ecological context: NDVI correlates positively with RH and SMI, and negatively with temperature, indicating that greener vegetation is associated with cooler and moister conditions. LAI shows similar but weaker correlations and is moderately associated with NDVI and dew point temperature, suggesting denser canopies tend to occur in more humid environments. Elevation shows a strong negative correlation with surface pressure (–0.90), consistent with atmospheric physics, and a positive correlation with distance to roads, indicating that higher areas are less accessible. Wind speed, slope, and curvature are largely uncorrelated with other features, suggesting they may contribute independent information to the modeling process. Overall, while some variables reflect shared physical processes, they also capture distinct ecological or spatial dimensions.

These findings suggest that later modeling steps should reduce redundancy and consider interaction effects. The correlation structure may also guide variable grouping or regularization strategies in models that are sensitive to multicollinearity.

2 Wildfire Danger Prediction

2.1 Missing values Handling

The quality and integrity of the dataset are fundamental to the reliability of the predictive modeling. Issues such as duplicates, anomalies, or missing values can introduce bias, reduce statistical power, and compromise model performance. Accordingly, careful attention was paid to ensure a clean and consistent dataset. No duplicate records were identified. Missing values, however, were present in six variables: **LST_day**, **LST_night**, **LAI**, **NDVI**, **SMI**, and **population**.

LST_day and LST_night were found to be highly correlated with t2m (air temperature at 2 meters), with correlation coefficients of $r = 0.94$ and $r = 0.96$, respectively. Given this strong linear relationship and the presence of missing values in both LST variables, they were excluded from the modeling dataset in favor of using t2m alone, which was complete. This decision avoided redundant information while preserving temperature-related variability relevant for fire prediction.

NDVI, LAI, and SMI were imputed using Last Observation Carried Forward (LOCF) or Next Observation Carried Backward (NOCB) for partially missing samples, while samples with all 30 days missing were removed. This decision was supported by the low within-sample variability and strong temporal autocorrelation, as summarized in Table 3.2. These characteristics indicated that values evolved gradually, without abrupt increases or decreases, making LOCF and NOCB appropriate and conservative imputation strategies that preserved the time-series structure.

Table 3.2: Within-sample temporal variability and lag-1 autocorrelation

Variable	Mean SD	Mean Range	Lag-1 ACF
NDVI	0.025	0.066	0.81
LAI	0.210	0.580	0.79
SMI	0.033	0.096	0.82

Source: Produced by the author using `LaTeX`

Finally, population was missing in two samples across all 30 days. As this variable is static and no auxiliary data were available to infer plausible values, these samples were removed entirely to avoid speculative imputation.

In summary, all missing data treatments were selected to maintain temporal integrity and minimize imputation bias while preserving as much valid data as possible for modeling. Since all imputations were performed independently within each sample using only its own time series, these operations did not risk information leakage and were safely applied prior to data splitting. The final dataset consisted of 676,230 rows, corresponding to 22,541 samples.

2.2 Temporal Data Splitting

To ensure a realistic and leakage-free evaluation, the dataset was divided into three time-based subsets: a training set covering 2006–2019, a validation set for the year 2020, and a test set spanning 2021–2022. This strictly forward-in-time split reflects the operational scenario where past data is used to predict future fire events.

Since each sample is a 30-day sequence of input data ranging from day $t-30$ to $t-1$, the prediction day falls immediately after the final observation day. To assign each sample to the correct temporal split based on its prediction day, a proxy ignition date, denoted as *t_day*, was computed as the latest date in the sequence plus one day.

$$t\_day = \max(time) + 1$$

This ensures that the temporal split aligns with the target day, preventing misassignment of samples across splits and avoiding temporal leakage.

Based on the computed *t_day*, the samples were partitioned as follows:

- **Training set (2006–2019)**: 16,370 samples (5,512 fire, 10,858 no fire)
- **Validation set (2020)**: 2,204 samples (751 fire, 1,453 no fire)
- **Test set (2021–2022)**: 3,967 samples (1,349 fire, 2,618 no fire)

2.3 Feature Engineering and Data Preprocessing

To prepare the dataset for deep learning, three key preprocessing steps were applied: the derivation of the Vapor Pressure Deficit (VPD), a well-established indicator of atmospheric dryness and fire danger commonly used in wildfire prediction studies; the normalization of continuous variables; and finally, data reshaping. We avoided upsampling to preserve the natural class imbalance and ensure that the model is trained under conditions that mirror real-world wildfire occurrence patterns, thereby supporting more realistic and operationally relevant performance.

Vapor Pressure Deficit (VPD) was computed using the 2-meter air temperature (t2m) and 2-meter dew point temperature (d2m). Both variables were first converted from Kelvin to Celsius. Saturation vapor pressure (e_s) and actual vapor pressure (e_a) were then calculated using the Tetens formula (same numbers as the mesogeos paper), and VPD was obtained as their difference:

$$VPD = e_s - e_a$$

This formulation captures the atmospheric water demand and is considered a physically meaningful predictor of vegetation stress and wildfire risk. After computing VPD, intermediate variables were discarded to maintain a compact and focused dataset.

Normalization was applied to ensure that all input variables contributed comparably to model training. A standardization approach was used, where each feature was transformed to have a zero mean and unit variance. The transformation was fitted exclusively on the training set to prevent data leakage and then applied consistently to the validation and test sets. Categorical and spatial identifier columns (e.g., x, y, land cover proportions) were excluded from this step. This approach preserves the statistical integrity of the evaluation pipeline by preventing information from future data from influencing the scaling parameters.

Reshaping for LSTM was performed to convert the splits into the required format for sequential modeling. They were reshaped into a 3D tensor of shape $(N, 30, F)$, where N is the number of samples, 30 is the number of time steps, and F is the number of features. This format enables the LSTM to capture temporal dependencies across the 30-day input window.

2.4 Model Training and Evaluation

Training

The binary classification task was addressed using a Long Short-Term Memory (LSTM) neural network architecture designed to capture sequential dependencies in the 30-day time series inputs. The model architecture comprised two stacked LSTM layers, each with **128 hidden units** and a **dropout rate of 0.2** to mitigate overfitting. The final hidden state from the last time step was passed to a fully connected layer with a single output neuron, followed by a sigmoid activation function to produce probabilities of fire occurrence.

The model was trained using the **binary cross-entropy loss function**, optimized with the **Adam optimizer** at a **learning rate of 0.001**. Training proceeded for up to **15 epochs**, and a **batch size of 64** was used to balance computational efficiency and training stability.

Model performance was evaluated using multiple metrics: accuracy, area under the receiver operating characteristic curve (AUC), and precision-recall curve (AUPRC), as well as precision, recall, and F1 score. These metrics were computed at the end of each epoch on the training set.

Validation Performance

On the validation set, the model achieved approximately a loss of **0.27**, with **accuracy** of **0.88**, **AUC** of **0.94**, and **AUPRC** of **0.90**. The **precision** and **recall** scores were **0.84** and **0.83**, respectively, resulting in an **F1 score** of **0.83**.

Test Performance

On the test set, multiple classification thresholds were explored. While several thresholds offered satisfactory trade-offs, a value of **0.24** was selected for final evaluation. This choice prioritized **recall**, which reached **0.8755**, without sacrificing precision excessively (**0.7579**), given that **false negatives (missed wildfires) are substantially more costly than false positives (false alarms)** in real-world fire management.

Figure 3.11: Precision, Recall, and F1 vs. Threshold

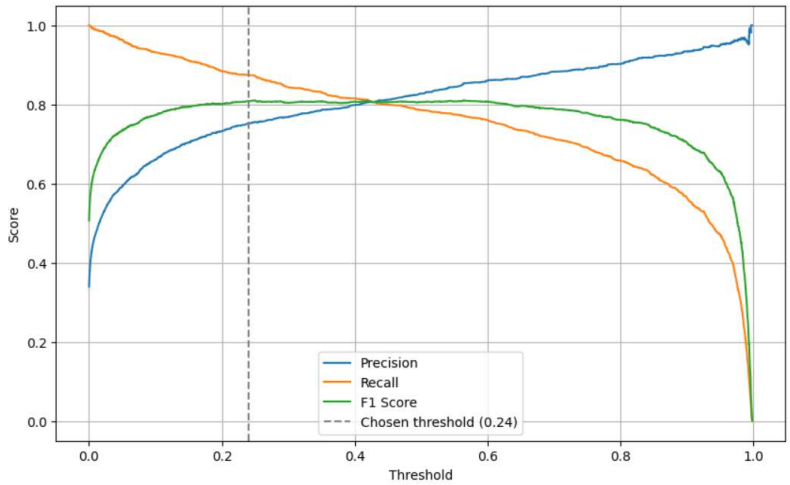

Source: Produced by the author using `Python`

Under this threshold, the model achieved a test loss of **0.3150**, an **accuracy** of **0.8573**, an **AUC** of **0.9379**, and an **AUPRC** of **0.8910**. The corresponding **F1 score** was **0.8067**, indicating a well-balanced performance between precision and recall.

2.5 Model Interpretability

2.5.1 Integrated Gradients.

We use Integrated Gradients (IGs) to generate temporal attribution plots for the input features (Figure 3.12). Given that our data spans a 30-day time window, IGs allow us to quantify the contribution of each feature to the model's predicted ignition probability at each individual time step. This enables us to visualize how the relevance of each variable evolves over time. In the context of wildfire risk prediction, such temporal attribution is particularly valuable, as it helps identify which conditions are most influential **and when**, thus supporting early warning and targeted prevention strategies.

Using normalized attribution values, the analysis enables direct comparison between features, identifying both dominant drivers and their temporal patterns, whether as early indicators or immediate triggers. Positive attributions indicate a feature's contribution to increasing fire probability, while negative values suggest a fire-suppressing effect. By focusing solely on fire samples, these plots decode the model's logic, validating its alignment with physical mechanisms or exposing potential biases.

The most salient pattern across the attribution plots is the sharp change observed in nearly all variables during the final week before ignition, following relatively stable contributions over the preceding weeks. This temporal transition suggests that the model relies more heavily on short-term signals when estimating ignition risk, an insight consistent with the physical dynamics of wildfire occurrence, where recent conditions are often decisive.

Meteorological features exhibit the highest attribution scores, underscoring their central role in ignition prediction. In particular, relative humidity (rh), vapor pressure deficit (vpd), temperature at 2 meters (t2m), total precipitation (tp), solar radiation (ssrd), surface pressure (sp), and wind speed all show sharp increases in positive attribution during the last week. This pattern reflects the typical contribution of hot, dry, and windy conditions to wildfire risk, as these factors promote vegetation desiccation and increase flammability.

In contrast, dew point temperature (d2m) and soil moisture index (smi) display negative attributions near ignition, suggesting that drier atmospheric and soil conditions are strongly associated with increased fire risk. These inverse relationships align with ecological understanding: reduced soil and air moisture levels reduce vegetation hydration, making ignition more likely.

Wind direction shows a weak decreasing attribution, reflecting its limited direct influence on ignition, but it has a vital role in fire spread.

Among **vegetation-related features**, the normalized difference vegetation index (ndvi) shows a predominantly negative attribution throughout the month, followed by a sharp increase during the final week. This may reflect a shift from moist green cover suppressing ignition early on, to contiguous cured fuels becoming available near the ignition date. The leaf area index (lai) maintains a weakly negative attribution, suggesting that denser canopies may modestly suppress fire risk, possibly due to increased shading or retained moisture.

Figure 3.12: Temporal Attribution Plots

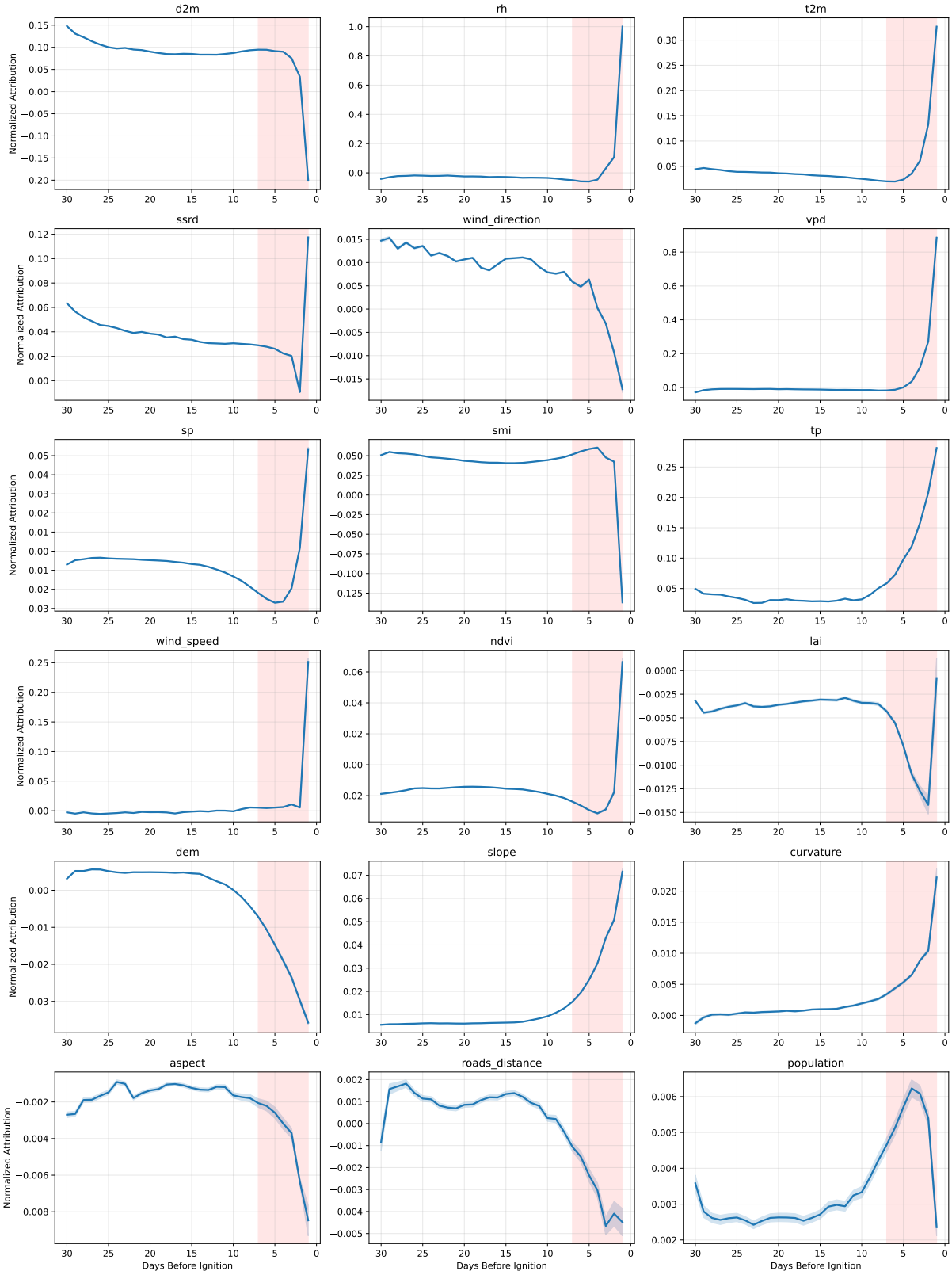

Source: Produced by the author using `Python`

Within the **Topographic and Anthropogenic Variables**, slope and curvature exhibit a positive attribution peak in the last few days, suggesting that steep and convex terrains contribute to higher ignition probability, potentially by accelerating wind-driven spread or concentrating solar radiation. In contrast, elevation (dem) shows a negative attribution, indicating that higher altitudes are associated with reduced fire risk, likely due to cooler temperatures, increased humidity, or remoteness from human activity.

Other variables, such as aspect, distance to roads, and population, display low-magnitude and fluctuating attributions. Slight negative attribution for aspect may correspond to north-facing slopes in the Mediterranean being less fire-prone due to moisture retention. A weak negative attribution for road distance suggests that proximity to roads increases fire likelihood, consistent with anthropogenic ignition sources. Population shows a mild positive attribution, indicating a small but present contribution of human presence to ignition risk, though it is less influential than meteorological drivers.

Summary Overall, these IG-based temporal attribution plots highlight the model's reliance on short-term, high-impact precursors, particularly meteorological variables, when predicting wildfire ignition. Vegetation, topography, and anthropogenic factors play a more contextual role, modulating risk based on site conditions. This reinforces the ecological plausibility of the model's behavior and supports its suitability for operational early-warning systems in fire-prone landscapes.

2.5.2 Permutation Feature Importance

To complement the insights from Integrated Gradients, we applied Permutation Feature Importance (PFI) to assess the global relevance of each feature across the test set.

Figure 3.13: Permutation Feature Importance (AUPRC)

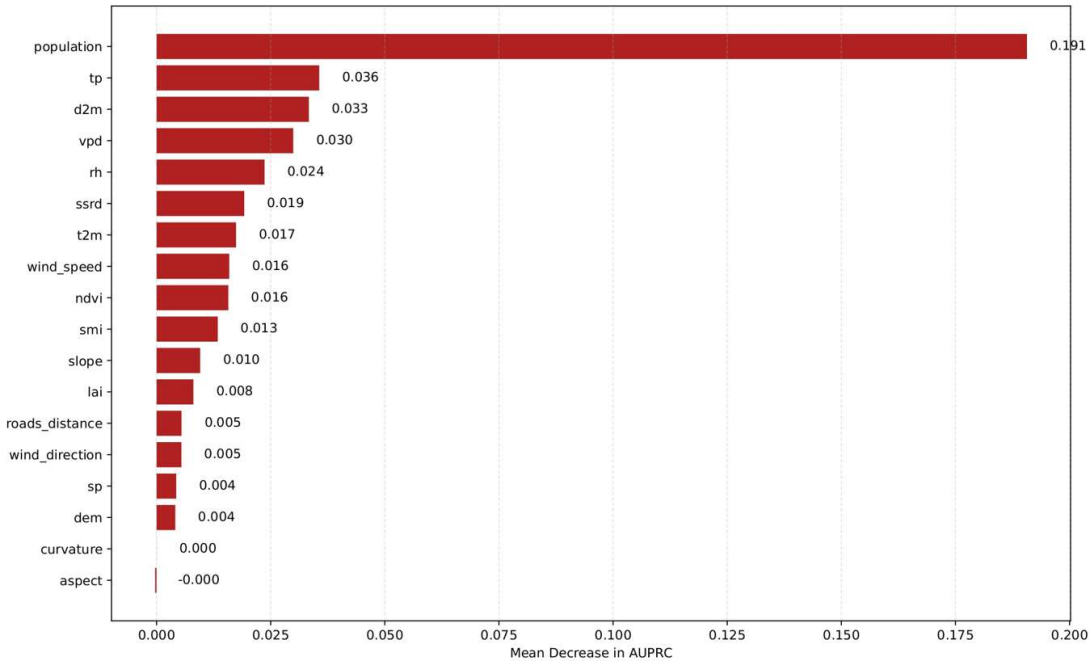

Source: Produced by the author using `Python`

As shown in Figure 3.13, PFI supports the insights derived from Integrated Gradients. Meteorological variables such as total precipitation (tp), dew point temperature (d2m), vapor pressure deficit (vpd), and temperature at 2 meters (t2m) are among the top-ranked features, reinforcing their critical role in predicting wildfire ignition. This alignment strengthens our confidence in the model's prioritizations.

Some differences do appear, however. Notably, population receives a much higher importance score under PFI compared to IGs, and features such as aspect and curvature are shown as negligible. These differences likely stem from methodological limitations of PFI, which evaluates each feature independently and does not account for interactions, spatial dependencies, or temporal dynamics.

Despite these caveats, PFI remains a useful complementary method. It offers an intuitive summary of global feature relevance and helps validate the core findings derived from IGs or other interpretability methods.

Conclusion

This chapter outlined the full wildfire prediction pipeline, from data preparation to model evaluation and interpretation. Using an LSTM trained on 30-day sequences, the model achieved a satisfying performance in predicting large fire ignitions, particularly in terms of recall and AUPRC.

Interpretability analysis using Integrated Gradients revealed that meteorological variables were the most influential, especially in the days leading up to ignition. Permutation Feature Importance supported these findings while providing a global view of feature relevance. Together, these results confirm the model's alignment with known fire-driving mechanisms and support its potential use in operational fire risk prediction.

General Conclusion

This dissertation has explored the application of Explainable Artificial Intelligence (XAI) and Long Short-Term Memory (LSTM) networks for wildfire risk assessment in the Mediterranean Basin, addressing the critical challenge of balancing predictive accuracy with interpretability in wildfire prediction. By integrating deep learning with interpretability techniques, this research contributes a novel framework that improves wildfire prediction and provides actionable insights for fire management.

Key Findings and Contributions

LSTM Performance and Predictive Capabilities

The LSTM-based model exhibited a strong performance by effectively capturing temporal dynamics in the data. Evaluation on the test set yielded an AUPRC of **89%** and a recall of **87.5%**, indicating a robust capability in identifying fire-prone conditions while minimizing false negatives, a critical requirement in early warning systems.

Validation of Research Hypotheses

Hypothesis 1: An LSTM-based model will outperform non-sequential models, due to its ability to learn and exploit temporal dependencies in the data

This hypothesis was not confirmed. While the LSTM successfully modeled sequential patterns, its overall performance was approximately equal to that of non-sequential models such as Random Forests when comparing the AUC metric.

Hypothesis 2: Interpretability techniques will reveal that short-term weather features are dominant predictors, aligning with known fire ecology.

This hypothesis was supported. Interpretability methods (Integrated Gradients and Permutation Feature Importance) consistently identified key variables such as temperature, relative humidity, and soil moisture as the most influential predictors of wildfire occurrence, aligning closely with established ecological understanding of wildfires.

Practical Implications

The proposed framework offers tangible benefits for wildfire management:

- It enables early detection of high-risk conditions, supporting proactive strategies such as pre-positioning firefighting resources or issuing targeted alerts.
- Interpretability results inform mitigation planning, guiding efforts like prioritizing prescribed burns in vulnerable vegetation zones or reinforcing firebreaks during drought conditions.

Limitations and Future Work

- While effective, the LSTM may not fully capture complex spatiotemporal interactions in the data. Future work could explore hybrid architectures, Graph Neural Networks (GNNs), or Transformer-based models, to better capture both spatial and temporal dependencies while also providing built-in explainability through attention mechanisms.

- Current interpretability outputs provide useful insights but remain limited. Employing more advanced XAI techniques, such as SHAP instead of PFI, could yield better and more detailed interpretations.

Final Reflection

As climate change intensifies wildfire risk across the Mediterranean and beyond, there is an urgent need for predictive tools that are both accurate and interpretable. This dissertation demonstrates that advanced AI models, when combined with domain expertise and explainability techniques, can bridge this gap, transforming complex environmental data into actionable knowledge for decision-makers.

Ultimately, this research demonstrates a promising path toward resilient, data-informed wildfire management, where AI does not merely anticipate disasters but actively contributes to their prevention.

Appendix

QR code linking to the Github repository containing all the code used in this dissertation.

References

Abdullah, T. A. A., Zahid, M. S. M., & Ali, W. (2021). A Review of Interpretable ML in Healthcare: Taxonomy, Applications, Challenges, and Future Directions. , *13*(12), 2439. Retrieved from https://www.mdpi.com/2073-8994/13/12/2439 doi: 10.3390/sym13122439

Apicella, A., Isgrò, F., & Prevete, R. (2024). *Don't Push the Button! Exploring Data Leakage Risks in Machine Learning and Transfer Learning*. Retrieved from http://arxiv.org/abs/2401.13796 doi: 10.48550/arXiv.2401.13796

Argüelles, C. R., & Collazo, S. (2023). Galaxy rotation curve fitting using machine learning tools. *Universe*, *9*. Retrieved from https://www.mdpi.com/2218-1997/9/8/372 doi: 10.3390/universe9080372

Benson, R. P., Roads, J. O., & Weise, D. R. (2008). Chapter 2 Climatic and Weather Factors Affecting Fire Occurrence and Behavior. In *Developments in Environmental Science* (Vol. 8, pp. 37–59). Elsevier. Retrieved from https://linkinghub.elsevier.com/retrieve/pii/S1474817708000028 doi: 10.1016/S1474-8177(08)00002-8

Breiman, L. (2001). Random forests. *Machine learning*, *45*, 5–32. Retrieved from https://link.springer.com/article/10.1023/A:1010933404324 doi: 10.1023/A:1010933404324

Cattau, M. E., Wessman, C., Mahood, A., & Balch, J. K. (2020). Anthropogenic and lightning-started fires are becoming larger and more frequent over a longer season length in the U.S.A. , *29*(4), 668–681. Retrieved from https://onlinelibrary.wiley.com/doi/10.1111/geb.13058 doi: 10.1111/geb.13058

Chekroun, S. (2009). *Commande neuro-floue sans capteur de vitesse d'une machine asynchrone triphasée* (phdthesis).

Chollet, F., Kalinowski, T., & Allaire, J. J. (2022). *Deep learning with R* (Second edition ed.). Manning Publications Co.

Chuvieco, E., Yebra, M., Martino, S., Thonicke, K., Gómez-Giménez, M., San-Miguel, J., … Viegas, D. (2023). Towards an Integrated Approach to Wildfire Risk Assessment: When, Where, What and How May the Landscapes Burn. , *6*(5), 215. Retrieved from https://www.mdpi.com/2571-6255/6/5/215 doi: 10.3390/fire6050215

Doshi-Velez, F., & Kim, B. (2017). *Towards A Rigorous Science of Interpretable Machine Learning*. Retrieved from http://arxiv.org/abs/1702.08608 doi: 10.48550/arXiv.1702.08608

Farid, A., Alam, M. K., Goli, V. S. N. S., Akin, I. D., Akinleye, T., Chen, X., ... Winkler, J. (2024). A Review of the Occurrence and Causes for Wildfires and Their Impacts on the Geoenvironment. , *7*(8), 295. Retrieved from https://www.mdpi.com/2571-6255/7/8/295 doi: 10.3390/fire7080295

Food, & Organization, A. (2007). *Fire management – global assessment 2006* (Vol. 151). Food and Agriculture Organization of the United Nations. Retrieved from https://www.fao.org/4/a0969e/a0969e00.htm

Food, & Organization, A. (2024). *Integrated fire management voluntary guidelines – principles and strategic actions. second edition.* (No. 41). (https://doi.org/10.4060/cd1090en)

Fromm, M., Lindsey, D. T., Servranckx, R., Yue, G., Trickl, T., Sica, R., ... Godin-Beekmann, S. (2010). The Untold Story of Pyrocumulonimbus. , *91*(9), 1193–1210. Retrieved from https://journals.ametsoc.org/doi/10.1175/2010BAMS3004.1 doi: 10.1175/2010BAMS3004.1

García-Redondo, C., Díaz-Raviña, M., & Regos, A. (2024). Long-term cumulative effects of wildfires on soil-vegetation dynamics in the "baixa limia–serra do xurés" natural park. *Spanish Journal of Soil Science, Volume 14 - 2024*. Retrieved from https://www.frontierspartnerships.org/journals/spanish-journal-of-soil-science/articles/10.3389/sjss.2024.13103 doi: 10.3389/sjss.2024.13103

Gupta, B., Agrawal, G., & Chauhan, A. (2022). *Forest fire: Characteristics and management*. Studera Press.

Haibo He, & Garcia, E. (2009). Learning from Imbalanced Data. *IEEE Transactions on Knowledge and Data Engineering*. Retrieved from http://ieeexplore.ieee.org/document/5128907/ doi: 10.1109/tkde.2008.239

Hochreiter, S., & Schmidhuber, J. (1997). Long Short-Term Memory. , *9*(8), 1735–1780. Retrieved from https://ieeexplore.ieee.org/abstract/document/6795963 doi: 10.1162/neco.1997.9.8.1735

Huidobro, G., Giessen, L., & Burns, S. L. (2024). And it burns, burns, burns, the ring-of-fire: Reviewing and harmonizing terminology on wildfire management and policy. , *157*, 103776. Retrieved from https://linkinghub.elsevier.com/retrieve/pii/S1462901124001102 doi: 10.1016/j.envsci.2024.103776

Jahn, W., Urban, J. L., & Rein, G. (2022). Powerlines and wildfires: Overview, perspectives, and climate change: Could there be more electricity blackouts in the future? *IEEE Power and Energy Magazine*, *20*(1), 16-27. Retrieved from https://ieeexplore.ieee.org/document/9675048 doi: 10.1109/MPE.2021.3122755

Jain, P., Coogan, S. C., Subramanian, S. G., Crowley, M., Taylor, S., & Flannigan, M. D. (2020). A review of machine learning applications in wildfire science and management. , *28*(4), 478–505. Retrieved from https://cdnsciencepub.com/doi/10.1139/er-2020-0019 doi: 10.1139/er-2020-0019

Jolly, W. M., Cochrane, M. A., Freeborn, P. H., Holden, Z. A., Brown, T. J., Williamson, G. J., & Bowman,

D. M. J. S. (2015). Climate-induced variations in global wildfire danger from 1979 to 2013. , *6*, 7357. Retrieved from https://research.fs.usda.gov/treesearch/48648 doi: 10.1038/ncomms8537

Kampezidou, S. I., Tikayat Ray, A., Bhat, A. P., Pinon Fischer, O. J., & Mavris, D. N. (2024). Fundamental Components and Principles of Supervised Machine Learning Workflows with Numerical and Categorical Data. , *5*(1), 384–416. Retrieved from https://www.mdpi.com/2673-4117/5/1/21 doi: 10.3390/eng5010021

Keane, R. E. (2013). *Describing wildland surface fuel loading for fire management: a review of approaches, methods, and systems*. USDA Forest Service, Rocky Mountain Research Station. Retrieved from https://www.fs.usda.gov/rm/pubs_other/rmrs_2013_keane_r001.pdf

Keane, R. E. (2015). *Wildland Fuel Fundamentals and Applications*. Springer International Publishing. Retrieved from https://link.springer.com/10.1007/978-3-319-09015-3 doi: 10.1007/978-3-319-09015-3

Kondylatos, S., Prapas, I., Camps-Valls, G., & Papoutsis, I. (2023). *Mesogeos: A multi-purpose dataset for data-driven wildfire modeling in the Mediterranean.* Retrieved from http://arxiv.org/abs/2306.05144 doi: 10.48550/arXiv.2306.05144

Kumar, J., Dalal, N., & Sethi, M. (2024). *Hyperparameters in Deep Learning: A Comprehensive Review.* Retrieved from https://ijisae.org/index.php/IJISAE/article/view/6967?utm_source=chatgpt.com

Leavell, D., Berger, C., Fitzgerald, S., & Parker, B. (2017, August). *Fire science core curriculum: Promoting awareness, understanding, and respect of fire through knowledge of the science* (Tech. Rep. No. EM 9172). Oregon State University, Forestry and Natural Resources Extension Program. Retrieved from https://catalog.extension.oregonstate.edu/em9172

LeCun, Y., Bengio, Y., & Hinton, G. (2015). Deep learning. , *521*(7553), 436–444. Retrieved from https://www.nature.com/articles/nature14539 doi: 10.1038/nature14539

Lemberger, P., Batty, M., Morel, M., & Raffaëlli, J.-L. (2015). *Big data et machine learning*.

Lipton, Z. C. (2018). The mythos of model interpretability. , *61*(10), 36–43. Retrieved from https://dl.acm.org/doi/10.1145/3233231 doi: 10.1145/3233231

Lutes, D. C., Keane, R. E., & Caratti, J. F. (2009). A surface fuel classification for estimating fire effects. *International Journal of Wildland Fire*, *18*(7), 802-814. doi: https://doi.org/10.1071/wf08062

Madrzykowski, D. (2012). *Fire dynamics: The science of fire fighting* (Tech. Rep.). National Institute of Standards and Technology (NIST). Retrieved from https://www.ifsta.org/sites/default/files/fire-dynamics-madrzykowski-2012.pdf

Martell, D. L. (2015). A Review of Recent Forest and Wildland Fire Management Decision Support Systems Research. , *1*(2), 128–137. Retrieved from http://link.springer.com/10.1007/s40725-015-0011-y doi: 10.1007/s40725-015-0011-y

McLauchlan, K. K., Higuera, P. E., Miesel, J., Rogers, B. M., Schweitzer, J., Shuman, J. K., … Watts, A. C. (2020). Fire as a fundamental ecological process: Research advances and frontiers. , *108*(5), 2047–2069. Retrieved from https://besjournals.onlinelibrary.wiley.com/doi/10.1111/1365-2745.13403 doi: 10.1111/1365-2745.13403

Meier, S., Elliott, R. J., & Strobl, E. (2023). The regional economic impact of wildfires: Evidence from southern europe. *Journal of Environmental Economics and Management*, *118*, 102787. Retrieved from https://www.sciencedirect.com/science/article/pii/S0095069623000050 doi: https://doi.org/10.1016/j.jeem.2023.102787

Mienye, I. D., Swart, T. G., & Obaido, G. (2024). Recurrent Neural Networks: A Comprehensive Review of Architectures, Variants, and Applications. , *15*(9), 517. Retrieved from https://www.mdpi.com/2078-2489/15/9/517 doi: 10.3390/info15090517

Molnar, C. (2025). *Interpretable machine learning* (3rd ed.). Retrieved from https://christophm.github.io/interpretable-ml-book

Moritz, M. A., Batllori, E., Bradstock, R. A., Gill, A. M., Handmer, J., Hessburg, P. F., … Syphard, A. D. (2014). Learning to coexist with wildfire. , *515*(7525), 58–66. Retrieved from https://www.nature.com/articles/nature13946 doi: 10.1038/nature13946

Moritz, M. A., Morais, M. E., Summerell, L. A., Carlson, J. M., & Doyle, J. (2005). Wildfires, complexity, and highly optimized tolerance. , *102*(50), 17912–17917. Retrieved from https://pnas.org/doi/full/10.1073/pnas.0508985102 doi: 10.1073/pnas.0508985102

Nielsen, M. A. (2015). *Neural networks and deep learning* (Vol. 25). Determination press San Francisco, CA, USA. Retrieved from https://scholar.google.com/scholar?q=Nielsen,+M.+A.+(2015).+Neural+Networks+and+Deep+Learning,+volume+25.+Determination+press+San+Francisco,+CA,+USA.&hl=fr&as_sdt=0&as_vis=1&oi=scholart

Nwankpa, C., Ijomah, W., Gachagan, A., & Marshall, S. (2018). *Activation Functions: Comparison of trends in Practice and Research for Deep Learning*. Retrieved from http://arxiv.org/abs/1811.03378 doi: 10.48550/arXiv.1811.03378

Office, C. B. (2022). *Wildfires*. Retrieved from https://www.cbo.gov/system/files/2022-06/57970-Wildfires.pdf (Publication No. 57970)

Olah, C. (2015). *Understanding lstm networks*. https://colah.github.io/posts/2015-08-Understanding-LSTMs/. (Accessed: 2025-05-30)

Oliveras Menor, I., Prat-Guitart, N., Spadoni, G. L., Hsu, A., Fernandes, P. M., Puig-Gironès, R., … Armenteras Pascual, D. (2025). Integrated fire management as an adaptation and mitigation strategy to altered fire regimes. , *6*(1), 202. Retrieved from https://www.nature.com/articles/s43247-025-02165-9 doi: 10.1038/s43247-025-02165-9

Organization, W. M. (2025). *Wmo confirms 2024 as warmest year on record at about 1.55°c above pre-industrial level*. Retrieved from https://wmo.int/news/media-centre/wmo-confirms-2024-warmest-year-record-about-155degc-above-pre-industrial-level

Pausas, J. G., & Keeley, J. E. (2021). Wildfires and global change. , *19*(7), 387–395. Retrieved from https://onlinelibrary.wiley.com/doi/abs/10.1002/fee.2359 doi: 10.1002/fee.2359

Peng, J., Jury, E. C., Dönnes, P., & Ciurtin, C. (2021). Machine Learning Techniques for Personalised Medicine Approaches in Immune-Mediated Chronic Inflammatory Diseases: Applications and Challenges. , *12*, 720694. Retrieved from https://www.frontiersin.org/articles/10.3389/fphar.2021.720694/full doi: 10.3389/fphar.2021.720694

Prestemon, J. P., Hawbaker, T. J., Bowden, M., Carpenter, J., Brooks, M. T., Abt, K. L., … Scranton, S. (2013). *Wildfire Ignitions: A Review of the Science and Recommendations for Empirical Modeling.* Retrieved from https://www.fs.usda.gov/treesearch/pubs/42766 doi: 10.2737/SRS-GTR-171

Rahman, R. A., White, B., & Ma, C. (2024). The effect of growth, deforestation, forest fires, and volcanoes on indonesian regional air quality. *Journal of Cleaner Production*, *457*, 142311. Retrieved from https://www.sciencedirect.com/science/article/pii/S0959652624017591 doi: https://doi.org/10.1016/j.jclepro.2024.142311

Reiner, V., Pathirana, N. L., Sun, Y.-Y., Lenzen, M., & Malik, A. (2024). Wish You Were Here? The Economic Impact of the Tourism Shutdown from Australia's 2019-20 'Black Summer' Bushfires. , *8*(1), 107–127. Retrieved from https://link.springer.com/10.1007/s41885-024-00142-8 doi: 10.1007/s41885-024-00142-8

Rizza, J., Adlam, C., & Berger, C. (2022). Prescribed fire basics: Fire behavior [Computer software manual]. Retrieved from https://extension.oregonstate.edu/sites/extd8/files/documents/12581/osu-rx-modules-fire-behavior-0423.pdf

Sairi, A., Labed, S., & Miles, B. (2024). Advancements in Intelligent Technologies Approaches for Forest Fire Detection: A Comparative Study. Retrieved from http://dergipark.org.tr/en/doi/10.33904/ejfe.1482838 doi: 10.33904/ejfe.1482838

Saito, T., & Rehmsmeier, M. (2015). The Precision-Recall Plot Is More Informative than the ROC Plot When Evaluating Binary Classifiers on Imbalanced Datasets. , *10*(3), e0118432. Retrieved from https://dx.plos.org/10.1371/journal.pone.0118432 doi: 10.1371/journal.pone.0118432

Samborska, V., & Ritchie, H. (2024). *Wildfires.* Retrieved from https://ourworldindata.org/wildfires

San-Miguel-Ayanz, J., Durrant, T., Boca, R., Maianti, P., Libertà, G., Jacome Felix Oom, D., … Loffler, P. (2024). *Forest fires in europe, middle east and north africa 2023* (Tech. Rep. No. JRC139704). Luxembourg: Publications Office of the European Union. Retrieved from https://data.effis.emergency.copernicus.eu/effis/reports-and-publications/annual-fire-reports/Annual_Report_2023.pdf doi: 10.2760/8027062

Sarker, I. H. (2021). Deep Learning: A Comprehensive Overview on Techniques, Taxonomy, Applications and Research Directions. , *2*(6). Retrieved from https://link.springer.com/10.1007/s42979-021-00815-1 doi: 10.1007/s42979-021-00815-1

Silva, P., Carmo, M., Rio, J., & Novo, I. (2023). Changes in the Seasonality of Fire Activity and Fire

Weather in Portugal: Is the Wildfire Season Really Longer? , *2*(1), 74–86. Retrieved from https://www.mdpi.com/2674-0494/2/1/6 doi: 10.3390/meteorology2010006

Singh, S. (2022). "Forest fire emissions: A contribution to global climate change". , *5*, 925480. Retrieved from https://www.frontiersin.org/articles/10.3389/ffgc.2022.925480/full doi: 10.3389/ffgc.2022.925480

Smith, J. K., Huff, M. H., Hooper, R. G., Telfer, E. S., & Schreiner, D. S. (2000). *Wildland fire in ecosystems: Effects of fire on fauna* (General Technical Report No. RMRS-GTR-42-vol. 1). Ogden, UT: U.S. Department of Agriculture, Forest Service, Rocky Mountain Research Station. Retrieved from https://www.fs.usda.gov/rm/pubs/rmrs_gtr042_1.pdf

Sohil, F., Sohali, M. U., & Shabbir, J. (2022). *An introduction to statistical learning with applications in R*. Retrieved from https://link.springer.com/book/10.1007/978-1-0716-1418-1 doi: 10.1080/24754269.2021.1980261

Song, Y., Xu, C., Li, X., & Oppong, F. (2024). Lightning-Induced Wildfires: An Overview. , *7*(3), 79. Retrieved from https://www.mdpi.com/2571-6255/7/3/79 doi: 10.3390/fire7030079

Sullivan, A. L. (2017). Inside the Inferno: Fundamental Processes of Wildland Fire Behaviour: Part 2: Heat Transfer and Interactions. Retrieved from http://link.springer.com/10.1007/s40725-017-0058-z doi: 10.1007/s40725-017-0058-z

Sundararajan, M., Taly, A., & Yan, Q. (2017). Axiomatic Attribution for Deep Networks. In *Proceedings of the 34th International Conference on Machine Learning* (pp. 3319–3328). PMLR. Retrieved from https://proceedings.mlr.press/v70/sundararajan17a.html

Sutton, R. S., & Barto, A. G. (2015). *Reinforcement Learning: An Introduction*. Retrieved from https://web.stanford.edu/class/psych209/Readings/SuttonBartoIPRLBook2ndEd.pdf

Syphard, A. D., Keeley, J. E., Massada, A. B., Brennan, T. J., & Radeloff, V. C. (2012). Housing Arrangement and Location Determine the Likelihood of Housing Loss Due to Wildfire. , *7*(3). Retrieved from https://dx.plos.org/10.1371/journal.pone.0033954 doi: 10.1371/journal.pone.0033954

Tedim, F., & Leone, V. (2020). The Dilemma of Wildfire Definition: What It Reveals and What It Implies. , *3*. Retrieved from https://www.frontiersin.org/articles/10.3389/ffgc.2020.553116/full doi: 10.3389/ffgc.2020.553116

Terven, J., Cordova-Esparza, D. M., Ramirez-Pedraza, A., Chavez-Urbiola, E. A., & Romero-Gonzalez, J. A. (2024). Loss Functions and Metrics in Deep Learning. Retrieved from http://arxiv.org/abs/2307.02694 doi: 10.48550/arXiv.2307.02694

U.S. Joint Economic Committee. (2023, October). *Climate-exacerbated wildfires cost the u.s. between $394 to $893 billion each year in economic costs and damages.* Retrieved from https://www.jec.senate.gov/public/index.cfm/democrats/2023/10/climate-exacerbated-wildfires-cost-the-u-s-between-394-to-893-billion-each-year-in-economic-costs-and-damages

Vachula, R. S., Nelson, J. R., & Hall, A. G. (2023). The timing of fireworks-caused wildfire ignitions during the 4th of July holiday season. , *18*(9), e0291026. Retrieved from https://dx.plos.org/10.1371/journal.pone.0291026 doi: 10.1371/journal.pone.0291026

Xu, R., Yu, P., Abramson, M. J., Johnston, F. H., Samet, J. M., Bell, M. L., ... Guo, Y. (2020). Wildfires, Global Climate Change, and Human Health. Retrieved from https://www.nejm.org/doi/full/10.1056/NEJMsr2028985

Xu, Z., Li, J., Cheng, S., Rui, X., Zhao, Y., He, H., & Xu, L. (2024). *Wildfire Risk Prediction: A Review.* Retrieved from http://arxiv.org/abs/2405.01607 doi: 10.48550/arXiv.2405.01607

Zhang, J. (2019). *Gradient Descent based Optimization Algorithms for Deep Learning Models Training.* Retrieved from http://arxiv.org/abs/1903.03614 doi: 10.48550/arXiv.1903.03614